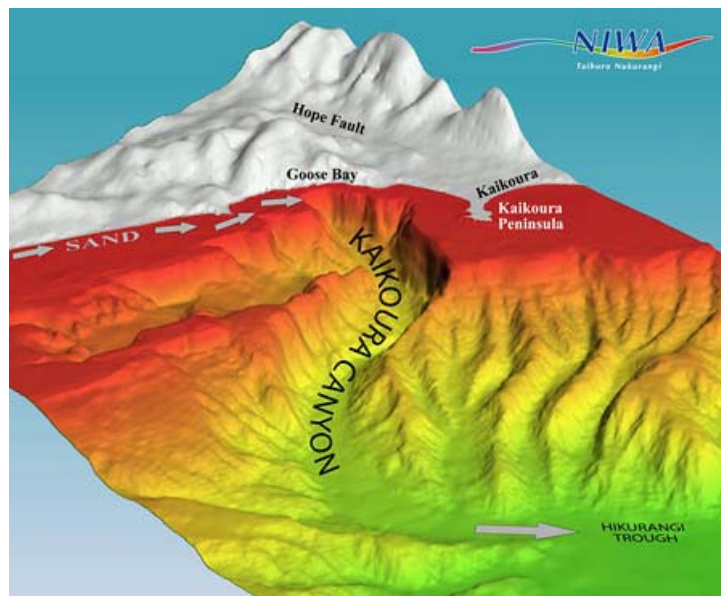


# KAIKOURA CANYON SUBMARINE LANDSLIDE DUE TO GROUND ACCELERATION GENERATED FROM THE HOPE FAULT



Francis Stewart  
Third Professional Year

A report submitted in partial fulfilment of the requirements for  
the BE (Hons) Degree in Natural Resources Engineering

Supervisor: Tim Davies  
Date Submitted: 4 October 2006

## **Executive Summary**

Sediment consisting of fine sand and silt is being deposited at the head of the Kaikoura Canyon near Goose Bay in the North East of the South Island, New Zealand. The deposit is located close to the coastline and has an estimated volume of 0.24km<sup>3</sup>. Slopes on the deposit are potentially unstable.

Peak ground accelerations in Kaikoura resulting from seismic activity have been estimated at 0.44g for a 150 year return period, which would cause a large amount of damage to infrastructure and some fatalities. This is also a plausible estimation of the magnitude of ground acceleration imposed on the sediment in the head of the Kaikoura Canyon.

The location of the sediment relative to coastal infrastructure such as roads and the relatively close proximity to houses to the shoreline makes the generation of a tsunami of significant size a real threat to the southern Kaikoura coastal area.

The conditions of the soil are largely unknown, and because of this, the behavioural characteristics under seismic perturbation are difficult to estimate. The behaviour of the soil was estimated by the model SLIDE 5.0 using values obtained from the literature which were used in landslide generation models that reproduced consistent landslide dynamics.

The undisturbed slope prism was stable but the initial unperturbed slope was shown to have a relatively low factor of safety. The introduction of a seismic force reduced the factor of safety of the slope, with the rate of reduction decreasing as the seismic load was increased. Seismic activity therefore created a significant reduction in slope stability.

Modelled failure occurred with a ground acceleration of 0.11g for the average slope, which is less than the estimated maximum predicted ground acceleration capable of being generated in the area of 0.44 g. Failure first occurred for the steepest section of the deposit at a ground acceleration of 0.08 g, which correlates to a Modified Mercalli Intensity V event.

## TABLE OF CONTENTS

<b>1.0</b>	<b>INTRODUCTION</b> .....	<b>5</b>
<b>2.0</b>	<b>BACKGROUND</b> .....	<b>6</b>
2.1	LOCATIONS.....	7
2.1.1	<i>Kaikoura Canyon</i> .....	7
2.1.2	<i>Hope Fault</i> .....	8
2.2	SEDIMENT .....	8
2.3	SEISMIC ACTIVITY .....	9
<b>3.0</b>	<b>MODEL GENERATION</b> .....	<b>10</b>
3.1	SLOPE DELINEATION .....	10
3.2	FAILURE PLANE DELINEATION .....	12
3.3	INITIAL CONDITIONS.....	13
<b>4.0</b>	<b>MODELLING</b> .....	<b>14</b>
4.1	SLIDE 5.0 SLOPE STABILITY PROGRAM.....	14
4.2	MODEL CREATION .....	14
4.2.1	<i>Slope With No Seismic Load</i> .....	16
4.2.2	<i>Slope With Maximum Seismic Loading</i> .....	19
4.2.3	<i>Deterministic Failure Event Analysis</i> .....	20
4.3	SENSITIVITY ANALYSIS .....	21
4.4	VARIATION IN SLOPE .....	25
<b>5.0</b>	<b>DISCUSSION</b> .....	<b>27</b>
<b>6.0</b>	<b>CONCLUSIONS AND RECOMMENDATIONS</b> .....	<b>29</b>
<b>7.0</b>	<b>ACKNOWLEDGEMENTS</b> .....	<b>30</b>
<b>8.0</b>	<b>REFERENCES</b> .....	<b>31</b>
<b>9.0</b>	<b>APPENDICES</b> .....	<b>35</b>
APPENDIX A	SLOPE DELINEATIONS FROM BATHYMETRIC CONTOURS FOR CROSS-SECTIONS .....	35
APPENDIX B	TABLE OF CONTOUR DELINEATION VALUES FOR SEDIMENT PRISM .....	38
APPENDIX C	MODEL OUTPUTS FOR HOMOGENEOUS & UNIFORM SOIL PROFILE SLOPES UNDER DIFFERENT GROUND ACCELERATION CONDITIONS .....	39
APPENDIX D	CHANGE IN SENSITIVITY OF MODEL PARAMETERS GIVEN A CHANGE OF SENSITIVITY RANGE .....	40

## LIST OF FIGURES

Figure 1 - Bathymetry of the Kaikoura Canyon and land topography .....	7
Figure 2 - The location of the Hope Fault (indicated in Red) in North Eastern Canterbury (Fruend 1971).....	8
Figure 3 – Potentially Unstable Sediment Mass at the Head of the Kaikoura Canyon (Region of Black Dashed Line) and Direction of Seismic Energy From the Hope Fault (Blue Arrow), with New Zealand Coast in Grey.....	9
Figure 4 - Slope Delineations (in Red) for the Sediment Deposit at the Head of the Kaikoura Canyon .....	10
Figure 5 – Cross-Section 2 of Sediment Prism: Northern Deposit Region as Shown in Fig. 4 ....	11
Figure 6 - Cross-Section 6 of Sediment Prism: Southern Deposit Region as Shown in Fig. 4.....	11
Figure 7 – Average of Cross-Section for the Sediment Prism .....	12
Figure 8 – A Hypothetical Representative Slope (brown line) Above a Failure Plane (red line) Showing the Stress Effects of the Column of Water Above the Sediment.....	13
Figure 9 Initial Cross-Section of Average Delineated Slope in SLIDE 5.0 with Homogeneous Soil Profile.....	15
Figure 10 Cross-Section of Average Slope in SLIDE 5.0 with Uniform Deposit Profile .....	15
Figure 11 Cross-Section of Average Slope in SLIDE 5.0 with Circular Tapered Deposit Profile..	16
Figure 12 Average Slope With Homogenous Soil Profile - Without Seismic Force .....	17
Figure 13 Average Slope in SLIDE 5.0 With Uniform Deposit Profile - Without Seismic Force....	17
Figure 14 Average Slope in SLIDE 5.0 With Circular Tapered Deposit Profile - Without Seismic Force.....	18
Figure 15 Average Slope in SLIDE 5.0 With Circular Tapered Deposit Profile – 0.44g Seismic Force.....	19
Figure 16 Interpolated Relationship Between Seismic Force and Minimum Factor of Safety .....	20
Figure 17 Sensitivity Plot for 0.114g Seismic Force on Average Slope .....	22
Figure 18 Sensitivity Plot for Seismic Force and Cohesion Relationship.....	23
Figure 19 Sensitivity Plot for Seismic Force and Angle of Internal Friction Relationship.....	24
Figure 20 Sensitivity Plot for Seismic Force and Unit Weight Relationship .....	24
Figure 21 Zones of Varying Stability Within the Sediment Deposit (From Table 4).....	26

**LIST OF TABLES**

Table 1 Seismic Force and Minimum Safety Factor Relationship ..... 20

Table 2 Modified Mercalli Intensity to Peak Ground Acceleration (PGA) Relationship  
(Mitalski 2006)..... 21

Table 3 Chosen Ranges of Values of the Model Parameters for Sensitivity Analysis .... 22

Table 4 Zones of Failure and the Relationship to Modified Mercalli Intensity and Ground  
Acceleration ..... 25

## 1.0 Introduction

The objective of this project is to determine the amount of sediment displaced in the Kaikoura Canyon from ground acceleration caused by an earthquake in the Hope Fault of differing moment magnitude. This will be done using a slope stability modelling program, with estimated soil parameters.

There have been many tsunamis along the New Zealand coastline in the last 100 years, 10 of which were greater than 5m in height (de Lange & Fraser 1999). NZ is heavily dependent on coastal infrastructure for transport, tourism and agriculture, as well as having most major cities and many townships on or near the coast, making it highly susceptible to significant damage as a result of a tsunami event.

Coastal roads and small townships in the Kaikoura coastal area, which are close to sea-level and are exposed to potential inundation, face significant risk if a tsunami is generated. Waves only a couple of meters high can still cause considerable damage to local infrastructure, as well as taking life. Predicted heights of tsunami waves generated from a landslide in the head of the Kaikoura Canyon reaching Oaro, a small coastal town, are up to 12 m, and these would arrive within a minute of the earthquake event and subsequent landslide (Walters et al, 2006).

The Kaikoura Canyon is part of an active conduit between a near-shore sediment transport system through the Conway Trough and the deep-ocean Hikurangi Channel (Lewis & Barnes 1999). The head of the canyon is within 500 m of the shoreline. Near shore sediment is the main source of sediment deposition in the canyon head, which acts as a sink for gravels, sand and mud.

The Hope Fault is one of the four major strike-slip faults of the Marlborough fault system and runs for 240 km from the Alpine Fault inland of Hokitika through North Eastern Canterbury to the coastline north of Kaikoura Peninsula.

A seismic event of significant size from the Hope Fault could trigger a submarine landslide in the Kaikoura Canyon. This is both historically and physically feasible given the active nature of the fault line and the large amount of unstable sediment accumulating at the head of the canyon. It is the potential instability at the head of the canyon that is the focus of this study.

This report gives background information on the Kaikoura Canyon and the Hope fault. It then outlines some of the sediment properties and the associated assumptions that pertain to the slope stability model. Then the steps used in order to generate the model are discussed, as well as the effect of ground acceleration on the slope stability, and the conditions in which failure occurs. The risk to the region associated with the likelihood of the modelled slope failure and the predicted effects from tsunamis is assessed.

## 2.0 Background

New Zealand is seismically very active, sitting on the convergence of the Australian and Pacific Plates along the 'Pacific Ring of Fire'. New Zealand historically has had many major earthquakes, as well as having minor events constantly and consistently throughout each year. There are predictions of an impending major seismic event generated from the Alpine Fault which could produce an event of Modified Mercalli Intensity X or greater; this may be a trigger for many landslides, both inland and submarine, to occur throughout the country. This event from the Alpine Fault rupture may in turn prompt seismic activity on associated faults such as the Hope Fault as well as throughout the country due to seismic energy propagation and other mechanisms (Robinson 2004).

Some of the largest tsunamis recorded were generated by submarine landslides (Trifunac & Todorovska 2002). These can also be driven by volcanic activity inducing gravity-driven mass flows (Pitman et al. 2002; Pitman et al. 2003) or more specifically the tremors and ground accelerations that accompany this activity. Flows in which fluid plays a significant role, as is the case for fully saturated soils like those assumed to occur in the Kaikoura canyon, typically have weaker interiors and are partly fluidised by pore pressure, as well as having high friction at the flow boundary (Denlinger & Iverson, 2001).

The peak tsunami amplitude for near-field generations depends on both the volume of displacement and the source velocity, in contrast to far field-field generations, as the initial pulse decreases due to dispersion (Todorovska 2002). Conversely; near-field tsunamis can have a larger amplitude under the same failure conditions due to the velocity pulse increasing the amplitude. As the Kaikoura Canyon deposit sits very close to the shore, the tsunami generated will be of a near-field nature.

Slide characteristics such as maximum slide velocity, initial acceleration, slide length, and thickness, all determine the characteristics of the tsunami. Effects of dispersion are usually not crucial to the final behaviour characteristics (Haugen et al. 2004), and the dispersion effects are less important in the near-field cases. Tsunamis produced from coseismic displacement are generally small as the wave amplitude is relative to the moment magnitude, whereas slope submarine landslides, once failure has occurred, can have displacements of many hundreds of meters regardless of the triggering earthquake magnitude (Grilli and Watts 2005).

The effects of a submarine landslide in terms of water disturbance depend heavily on the material density, the size and the depth of the sediments that are displaced (Watts et al. 2000; Liu et al. 2005). As there is not much data on the physical and behavioural characteristics of the deposit, many of the parameters have to be based on assumptions using typical soil properties.

Highly focussed waves can inundate small sections of coastline with high amplitudes (Fisher et al. 2004), as well as localised waves creating large run-ups, especially in bays and fjords (Hayir, 2003; Hayir 2006). This means that Goose and Oaro Bays are susceptible to increased wave heights from localised amplitude concentrations. This is of importance in regards to the population in the Oaro, which is considered to be low.

## 2.1 Locations

### 2.1.1 Kaikoura Canyon

The Kaikoura Canyon head is located 13km SW of the Kaikoura Peninsula and 1km east of Goose Bay (42 ° 29' S, 173 ° 32' E), as shown in Figure 1. It is 60 km long, up to 1200 m deep, and is generally U-shaped.

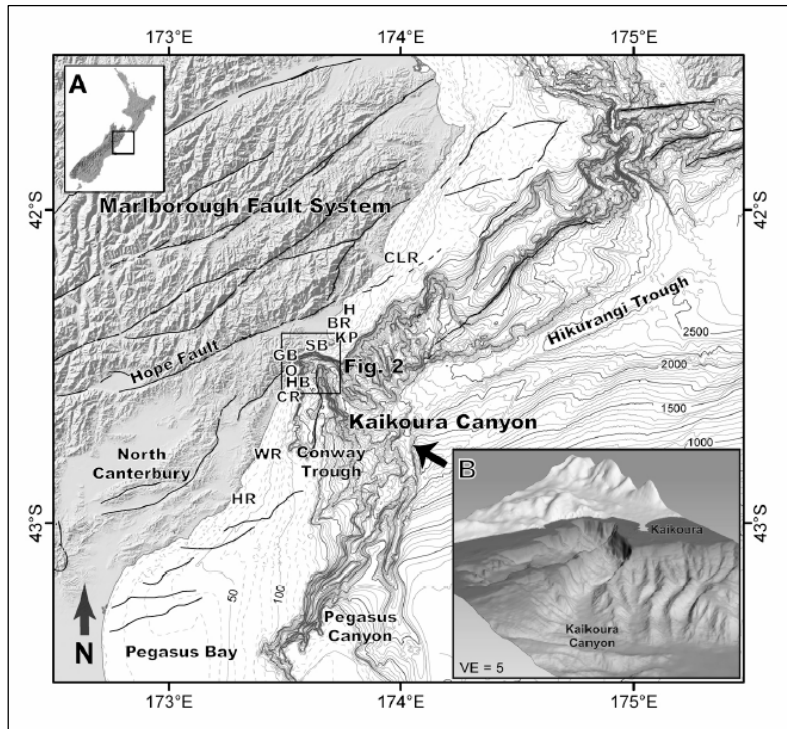


**Figure 1 - Bathymetry of the Kaikoura Canyon and land topography**

Bathymetry of the Kaikoura Canyon and land topography (main figure). Bathymetric contours in metres. Black lines are simplified tectonic faults. (CLR, Clarence River; H, Hapuku; BR, Beach Road; KP, Kaikoura Peninsula; SB, South Bay; GB, Goose Bay; O, Oaro; HB, Haumuri Bluffs; CR, Conway River; WR, Waiiau River; HR, Hurunui River.) Inset B is an oblique 3-D bathymetric view of Kaikoura Canyon viewed in the direction of the bold arrow on the main map (Walters et al. 2006)

This canyon is remote from the mouth of sediment laden rivers, and has been described as the sink for the coastal sediment transport system from the rivers that drain the South Island's rapidly rising mountains (Carter et al. 1979), which contrasts to some canyons which receive sediment directly from river systems.

The canyon head is located 500 m east of Goose Bay, and receives sediment from the east coast sediment transport system. The total sediment volume of  $240 \times 10^6 \text{ m}^3$  accumulating in the canyon head at around  $1.5 \times 10^6 \text{ m}^3$  per year (Walters et al. 2006; Lewis & Barnes 1999) means the sediment has been gathering for approximately the past 160 years (Walters et al. 2006). This short time period suggests that the sediment has been flushed down the canyon previously, which may have been partially due to similar submarine landslide events.

## 2.1.2 Hope Fault

The Hope Fault is one of the four major strike-slip faults of the Marlborough fault system and runs for 240 km starting from the Alpine Fault, inland of Hokitika (figure 2), across North Eastern Canterbury, and is only discernible as a single major fault for around 140 km.

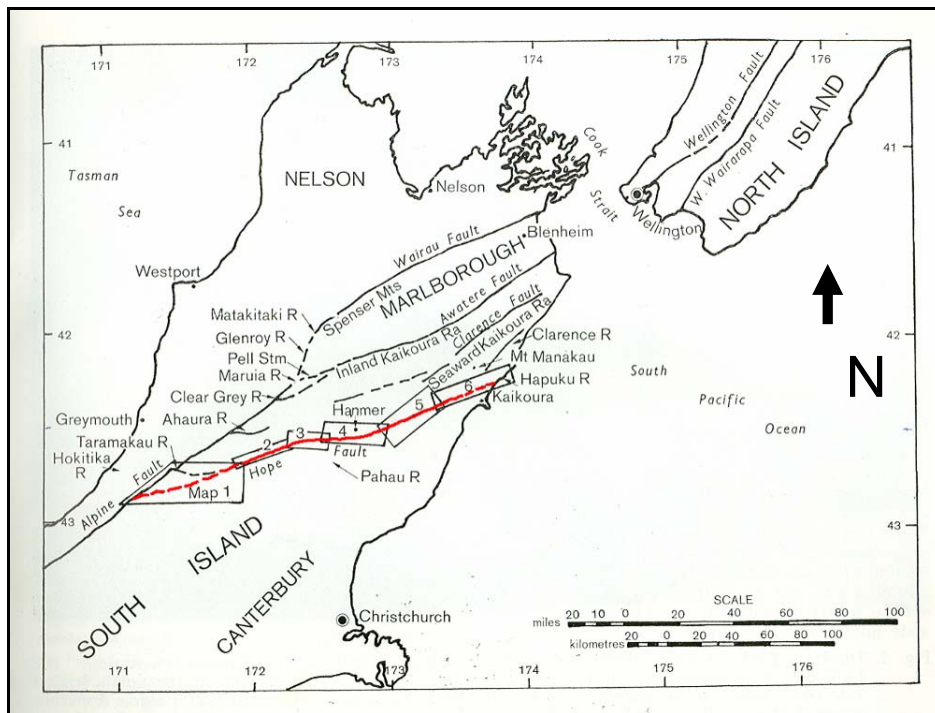
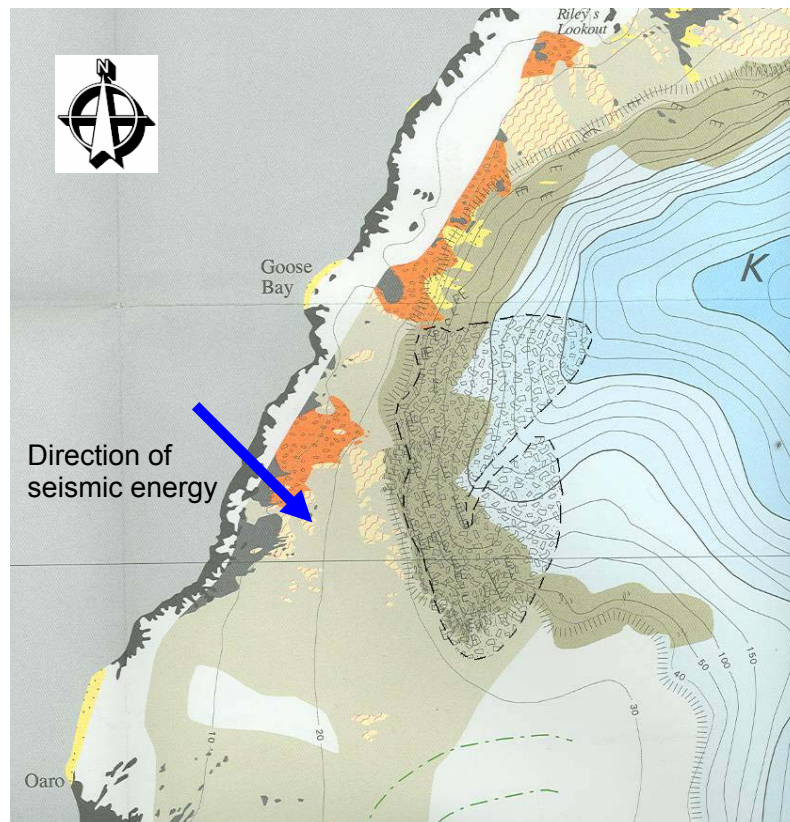


Figure 2 - The location of the Hope Fault (indicated in Red) in North Eastern Canterbury (Freund 1971)

There is evidence that this fault has displaced up to 12 miles laterally, with dextral offsets of up to 8.5 ft from the 1888 earthquake in the Hope River region (Freund 1971). The average dip-slip rate is less than 4 mm/year, and the section of the fault around the Kaikoura region may have a rate of uplift around 6 to 10 mm/year (van Dissen & Yeats 1991). This shows a reasonable amount of activity from the Hope Fault, both currently and historically.

## 2.2 Sediment

The sediments deposited in the headwater of the Kaikoura Canyon are mainly fine sands and silts, as most of the gravels are confined within the beach compartments (Lewis et al. 2006). They are assumed to be fully saturated, with a hydrostatic pressure distribution, and an angle of internal friction of  $33^\circ$  (Tim Davies pers. comm.), as well as being cohesionless (Wright & Rathje 2003). The sediment mass has settled in two distinctive sections (Figure 3), which are projecting into the canyon from two different orientations.



**Figure 3 – Potentially Unstable Sediment Mass at the Head of the Kaikoura Canyon (Region of Black Dashed Line) and Direction of Seismic Energy From the Hope Fault (Blue Arrow), with New Zealand Coast in Grey.**

Estimates for the soil density and friction coefficient parameters were  $1600 \text{ kg/m}^3$  ( $15.696 \text{ kN/m}^3$ ) and  $0.02 \text{ s}^{-1}$  respectively (Walters et al. 2006), which were values used in landslide generation models that reproduced consistent landslide dynamics (Fleming et al. 2005 in Walters et al. 2006). The specific density was assumed to be  $\gamma = 1.85$ , which is a generally typical value for similar soil types.

### 2.3 Seismic Activity

Under earthquake loading, the sediment movement behaviour is influenced by the intensity and duration of the cyclic loading and the state of the sediment (Sultan et al. 2004). This includes the grain size distribution, the percentage of clay, and the saturation condition.

The estimated 150 year return period peak ground acceleration that could occur in Kaikoura is  $0.44g$  (Stirling et al. 2002; Stirling et al. 2001 in Walters et al. 2006), correlating to a magnitude 8 earthquake on the Hope Fault. The seismic energy is assumed to travel perpendicular to the fault, as the location of the rupture could be anywhere along the fault line, and the energy radiates out from this site. This means the seismic waves will reach the Kaikoura Canyon from a north-west direction (as indicated in figure 3). And as the Hope Fault is Strike-Slip, and most of the energy will be from horizontal displacement, the horizontal ground acceleration was used in the model.

### 3.0 Model Generation

Tsunamis due to retrogressive slides are generally smaller than for a similar fixed shaped slide with the same characteristics due to an increased duration of slide mass mobilisation (Haugen et al. 2004). This is an assumption that is used for the slope failure mechanism.

The model will be built based on the physical bathymetry and the assumed properties for the sediment.

#### 3.1 Slope Delineation

The slope surface that was used for the model was generated by taking slope cross-sections from the Kaikoura Canyon: Depths, Shelf Texture and Whale Dives chart developed by NIWA (Lewis, K.B., Garlick, R.D. and Dawson, S.M. 1998), and determining a slope which would best represent the sediment deposit (figure 4). This was taking into account which slope would best represent the failure conditions for both of the two deposits, and account for the failure surface for much of the total sediment volume.

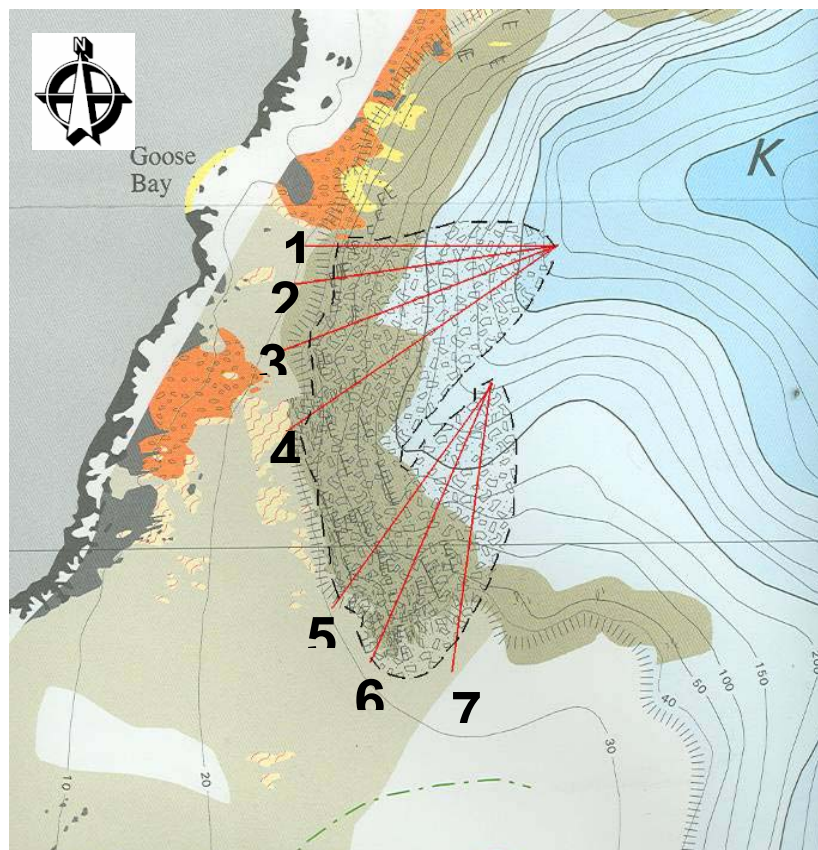


Figure 4 - Slope Delineations (in Red) for the Sediment Deposit at the Head of the Kaikoura Canyon

As there was no cross-section that clearly represented the whole deposit, and the marked differences in depth of the two regions of the sediment, two representative slopes were taken, one from each section, being cross-sections 2 and 6 for the respective regions (figures 5 & 6). The cross-sections were entered into the slope definition in the program SLIDE 5.0 to graphically show the slopes (note the change in scale):

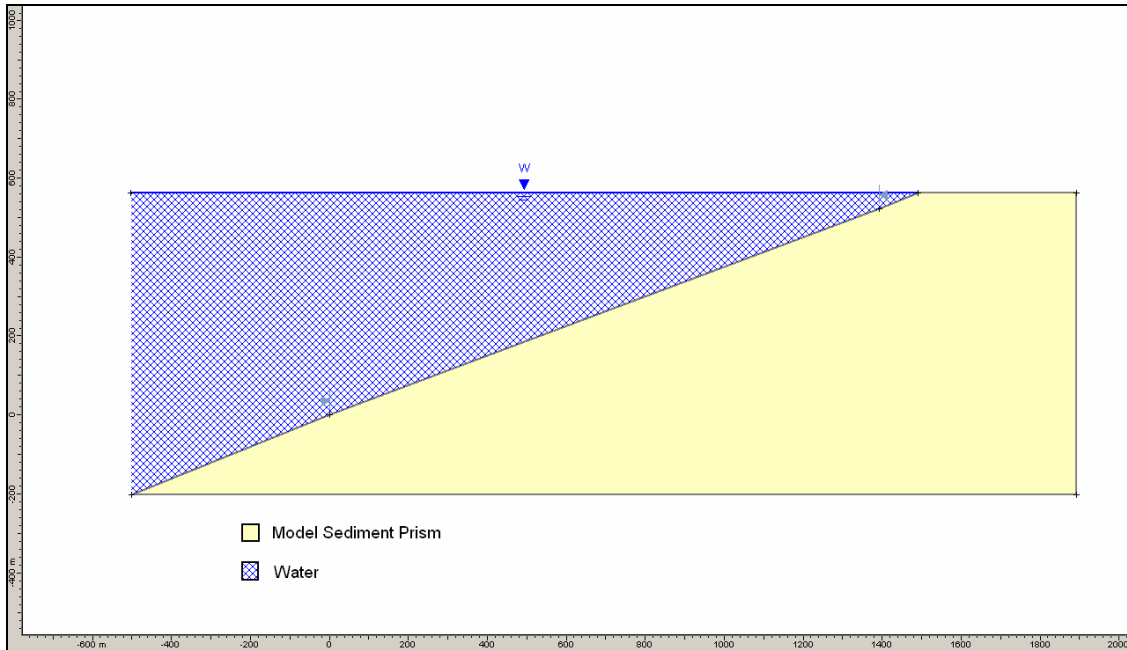


Figure 5 – Cross-Section 2 of Sediment Prism: Northern Deposit Region as Shown in Fig. 4

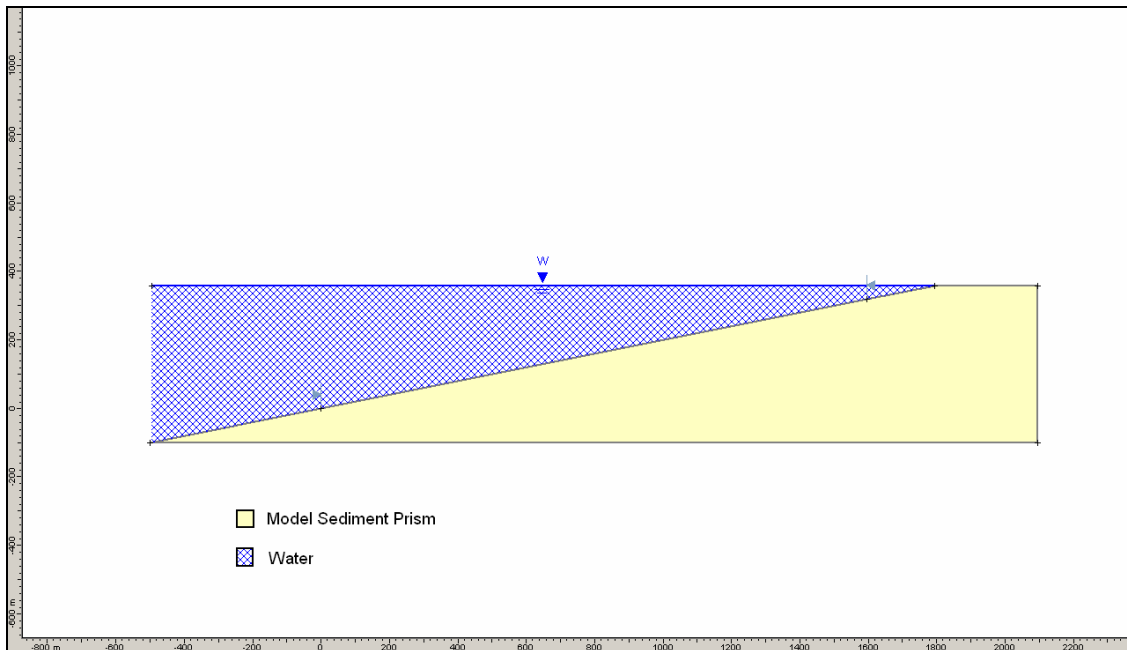
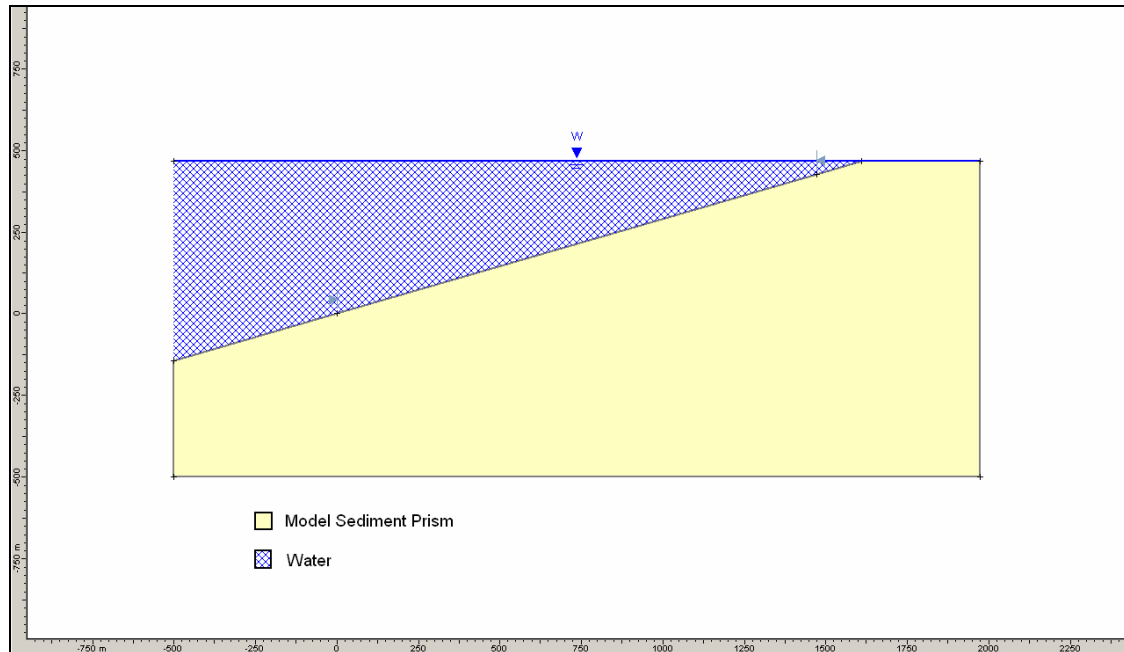


Figure 6 - Cross-Section 6 of Sediment Prism: Southern Deposit Region as Shown in Fig. 4

The average slope gradient and length was calculated for the whole deposit, from which a linear slope was developed (fig 7). This slope is not representative for the sediment deposit, but may be useful for result comparisons.



**Figure 7 – Average of Cross-Section for the Sediment Prism**

These are the slopes for which the modelling is parameterised.

The inferred of direction the seismic force propagation meant that only one section of the deposit can be feasibly modelled in two-dimensions (2-D), with a still slightly oblique wave approach. As the ground acceleration will add to instability in all directions, the obliquity of the seismic wave approach was initially assumed to be negligible. This is one of the reasons that a three-dimensional (3-D) model would be more accurate.

### **3.2 Failure Plane Delineation**

The failure plane below the deposit has been estimated to over 40m at its thickest, based on high resolution seismic profiles of the sediment area (Lewis & Barnes 1999). This is the criterion that will be used when delineating the failure planes, assumed to be circular, and tapering naturally at each extent of each cross-section. In order to test this for the purpose of the model, the sediment underlying the prism was assumed to have infinite strength, thus modelling the characteristic failure of the overlying sediment prism only.

### 3.3 Initial Conditions

The state of the pore pressures in the soil are related to the condition and behaviour of the water surface, which may become perturbed due to the ground accelerations. A relationship between the state of the free-water surface and the pore water pressure was postulated, whereby if the water remains fairly level there is no significant change in excess pore water pressure (Bowman, E. pers. comm.). It was assumed that the surface of the water remained relatively level during the initial stages of the ground movement, keeping hydrostatic conditions prior to the slope failure, as well as limiting the effects of excess pore pressure. This dependence of excess pore pressure on the behaviour leading to failure is partly due to whether it acts in a drained or un-drained manner, with the relationship between the stresses and the pore water pressure shown by the equation (1):

$$\sigma' = \sigma - U \quad (1)$$

Where  $\sigma'$  is the effective stress,  $\sigma$  is the total stress and  $U$  is the pore water pressure. The stress influencing the sediment is from the column of water above the soil, as shown in figure 6:

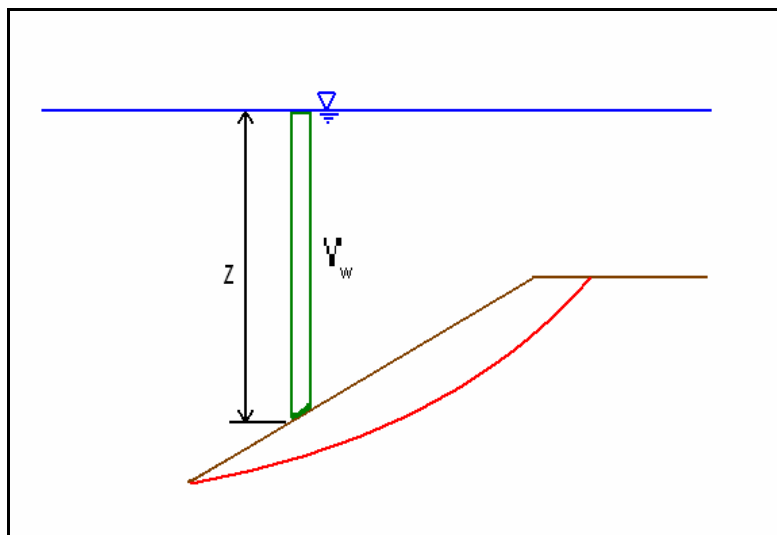


**Figure 8 – A Hypothetical Representative Slope (brown line) Above a Failure Plane (red line) Showing the Stress Effects of the Column of Water Above the Sediment**

This figure shows the effect of the water column (in green) with a density  $\gamma_w$  over a vertical depth  $z$  creating the total stress from the water  $\sigma$ .

This is time dependent because the soil can act in either a drained or undrained manner, and the length of the earthquake, both in terms of wavelength and duration, can differentially affect the motion of the ocean. The soil was assumed to act in a drained manner prior to the initial failure so as not to impose an excess pore pressure scenario.

## **4.0 Modelling**

### **4.1 SLIDE 5.0 Slope Stability Program**

SLIDE 5.0 is a 2D slope stability model which can evaluate both probabilistic and deterministic factors of safety for circular and non-circular failure surfaces in soil or rock slopes. The effects of external loading and seismic loading can be modelled also. Slip surfaces can be analysed individually, or search methods can be applied to locate the critical slip surface for a given slope.

The program has a Graphical User Interface (GUI) in which slopes, material layers, loads and water tables can be created. It also has a graphical output for the results showing failure planes and their factor of safety. There is also a sensitivity analysis capability within the program to determine the influence of variations in parameters on the model output.

The method used to determine failure slope and factor of safety was the program's deterministic approach, whereby the stability given a scenario was determined, rather than calculating the probability of the outcome.

### **4.2 Model Creation**

The slope section under consideration was delineated in the GUI using the average cross-section slope of the sediment prism for the measured slope length, with an additional 500 m either side. The average slope was used to initialise the model and gauge the slope stability and response to seismic energy exposure. It was also used to test the sensitivity of the model parameters.

The limits within which the model would operate were defined as the length of the deposit as taken from the bathymetric map. The water table was defined at sea level, and was assumed to have negligible vertical displacement prior to the seismic event.

The required material properties that were assumed for the model were the unit weight, the cohesion and Phi (the angle of internal friction.) The value for unit weight of 15.696 kN/m<sup>3</sup> was taken from Walters et al. 2006. Values of 0 kN/m<sup>2</sup> and 33° were assumed for the cohesion and angle of internal friction respectively. The model also assumes homogeneity of soil properties throughout each of the layers. The initial slope cross section is shown in figure 9.

As the sediment prism is thought to be a maximum of 40 m in depth from the high resolution seismic profiling, a second slope was created that had a uniform sediment layer throughout the slope with the material properties of those specified, as well as a third slope that had a curved cross-section with a maximum thickness of 40 m. The circular sediment deposit was created to emulate a more natural sediment stratigraphy.

The underlying layer material was given an infinite strength to gauge the influence of the underlying material on the behavioural response to seismic perturbation of the sediment of interest. This also tested the effect of different sediment prism dimension assumptions. These are shown in figures 10 & 11.

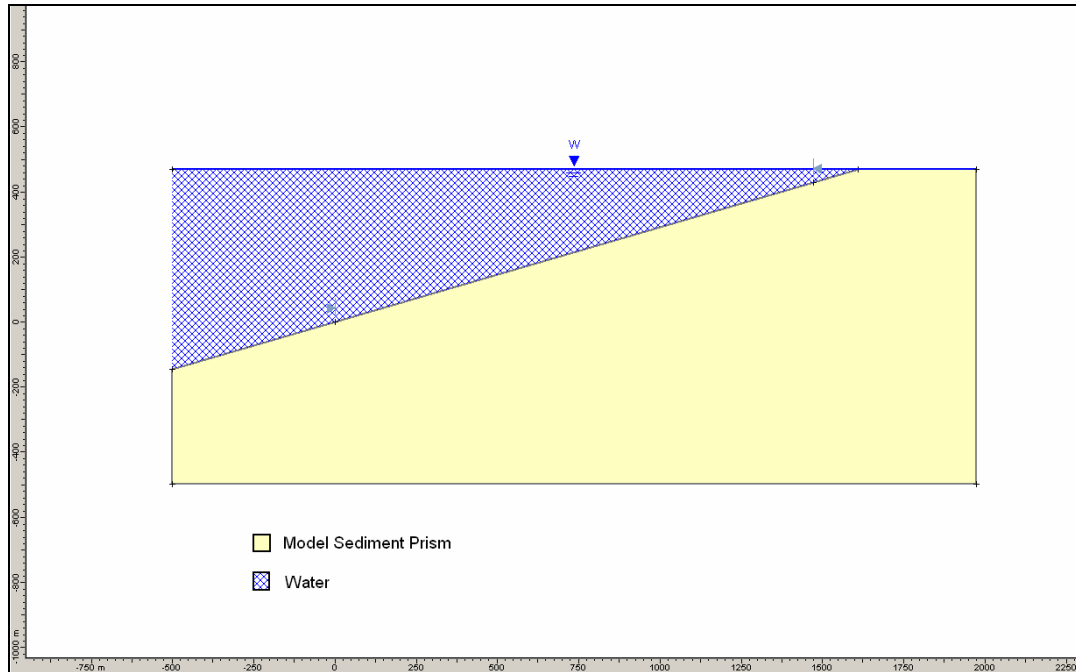


**Figure 9 Initial Cross-Section of Average Delineated Slope in SLIDE 5.0 with Homogeneous Soil Profile**

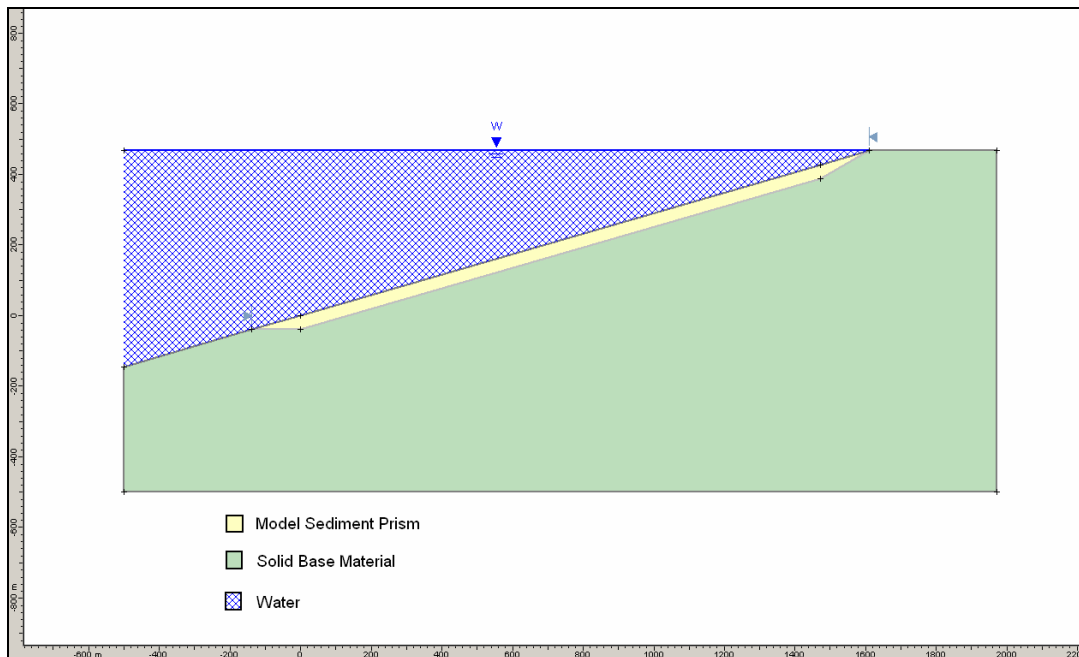


**Figure 10 Cross-Section of Average Slope in SLIDE 5.0 with Uniform Deposit Profile**

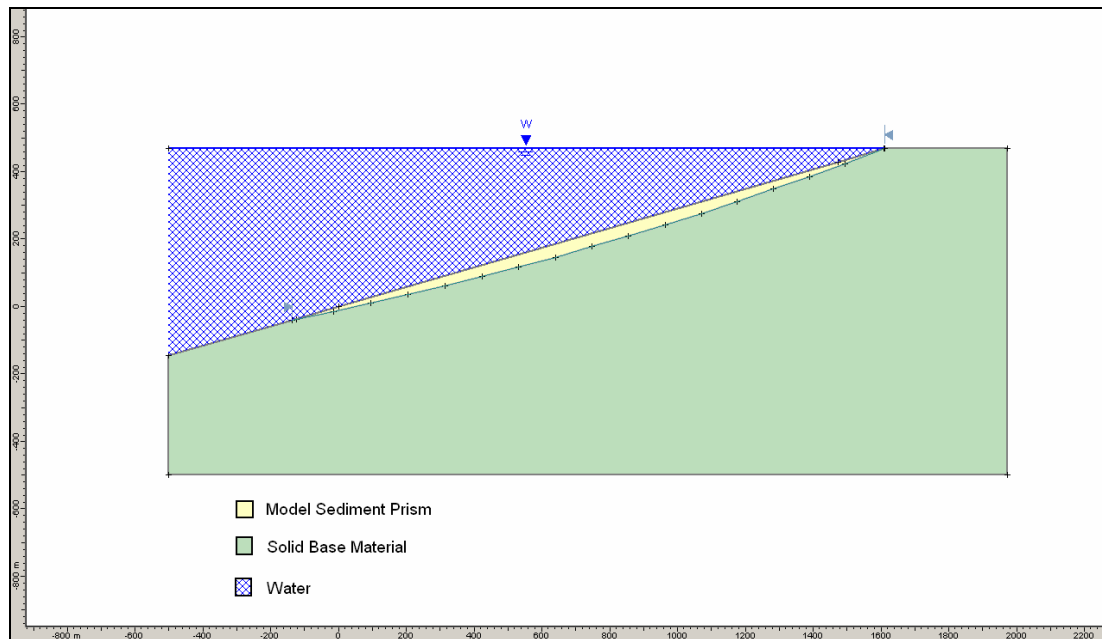


**Figure 11 Cross-Section of Average Slope in SLIDE 5.0 with Circular Tapered Deposit Profile**

As the modelling boundaries were defined for the slope, the layout of the slope above and below the focus area had no bearing on the result. This was tested by varying the up-slope and down-slope bathymetry (which was unknown) and gauging the effect on the slope stability, which was none.

#### 4.2.1 Slope with No Seismic Load.

The model was run with no external loads to assess the static stability of the slope. This was done by using the *Slope Search* method to determine the factor of safety for surfaces with each of the slope layers. This method defines failure surfaces with the only constraints being the defined slope limits and the number of user specified failure surfaces desired. They are radial failure planes which are tested for stability from an axis point above the slope, which is defined by the program. The number of specified surfaces was 5000, and was the default number of slope surfaces given by SLOPE 5.0. The minimum factor of safety of 2.2 for the slope was the output from unloaded slope scenario. This occurred over a short length in the middle of the slope (figure12). This means that even at the lowest factor of safety the slope will not fail given the current conditions. There was also a uniform increase in safety factor upon an increase in depth.

The same method was applied for the two slopes that had an underlying solid base. The same parameters gave the same factor of safety for the minimum surface for both of the two subsequent slopes (see figures 13 & 14).

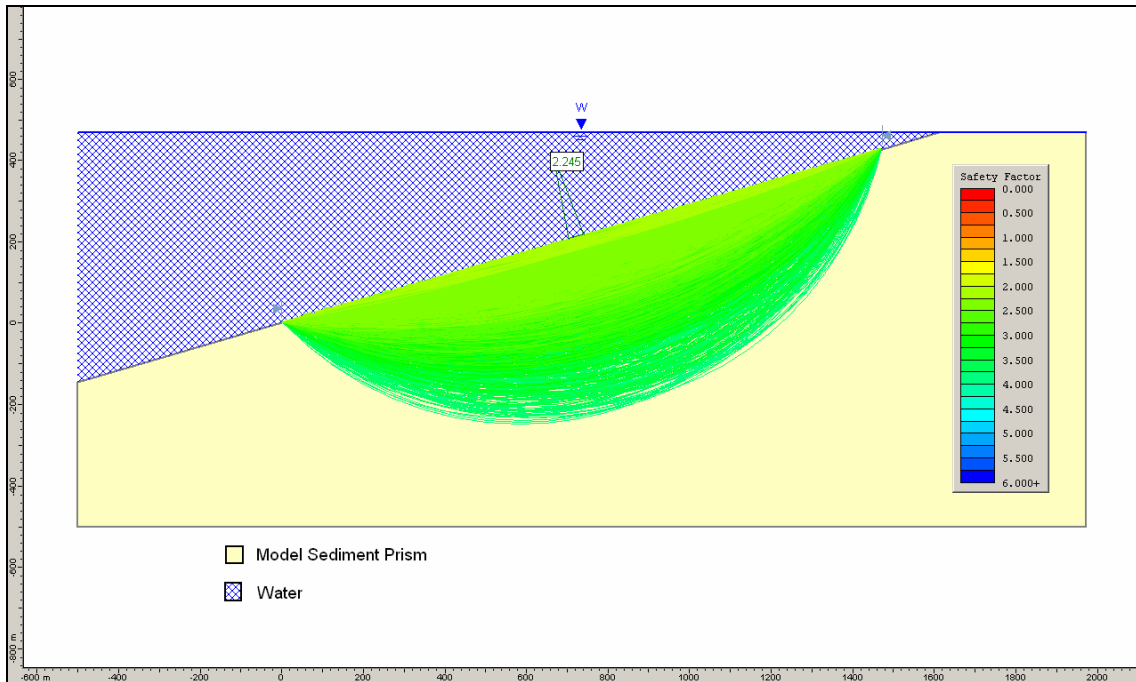


Figure 12 Average Slope With Homogenous Soil Profile - Without Seismic Force

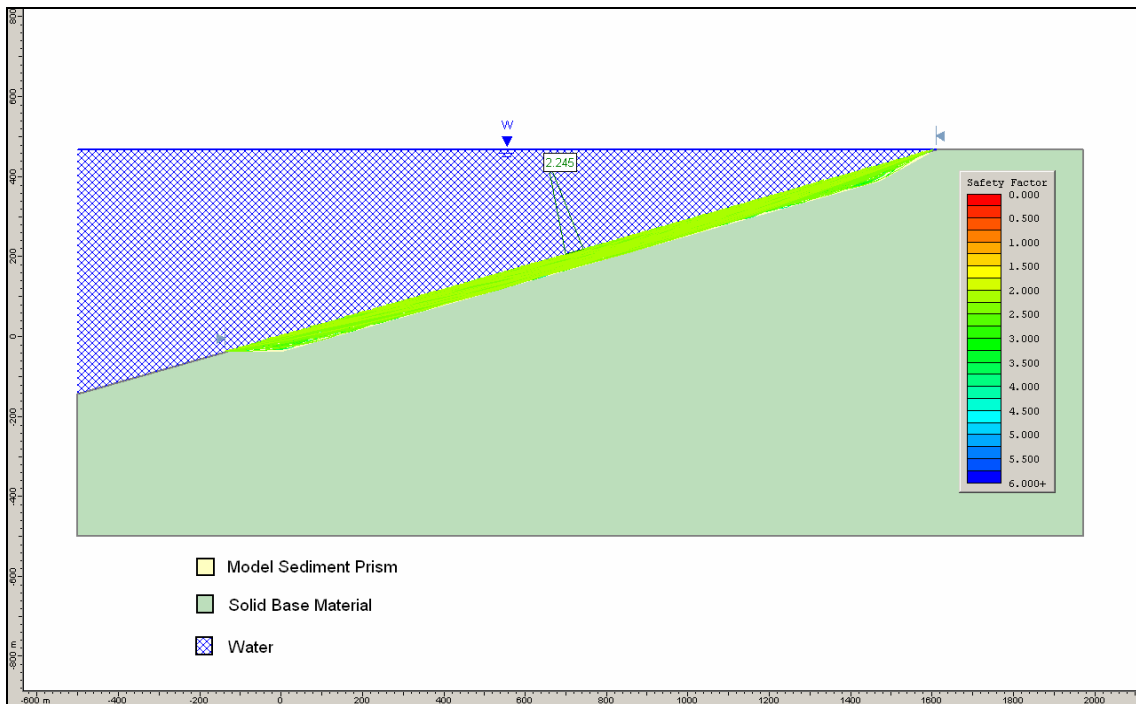
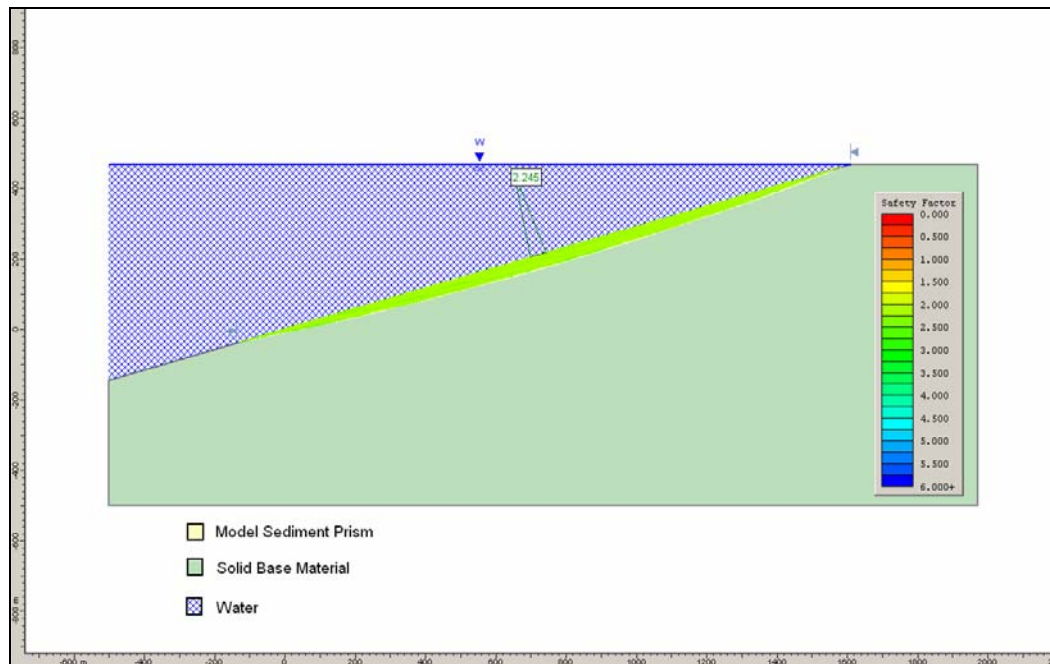


Figure 13 Average Slope in SLIDE 5.0 With Uniform Deposit Profile - Without Seismic Force



**Figure 14 Average Slope in SLIDE 5.0 With Circular Tapered Deposit Profile - Without Seismic Force**

This shows the same increase in safety factors with depth. This allows for two important assumptions to be made for this model:

1. The underlying material does not influence the stability of the overlying layer,
2. The safety factor is the same along each of the radial failure planes, which become more stable as the depth of the failure plane increases (i.e. increases in factor of safety).

The significance of the first assumption is that more accurate investigation of the properties of the underlying material is not necessary for this analysis as it does not significantly affect the critical failure surface. This does not address the inter-layer interaction affecting the failure mechanism and friction interactions that are not investigated in this report.

The second assumption means that if there is a critical failure mode attained at the maximum depth of 40 m, then failure will happen for the whole sediment deposit. This means that an event that reduces the factor of safety for the base of the layer to less than 1 will cause the whole slope to fail at once. As the factor of safety for all of the failure surface layers within the 40 m depth for the deposit are approximately the same, the sediment deposit will fail as a unit.

## 4.2.2 Slope with Maximum Seismic Loading

The tapered slope was used as the representative slope for the rest of the analysis based on the assumptions made from the first set of results. The behaviour of the homogenous and uniform soil profile slopes was the same, with model outputs shown in Appendix C.

Seismic forces are dimensionless coefficients which represent the earthquake ground acceleration as a fraction of the acceleration due to gravity. The maximum seismic loading that was assumed to be generated from the Hope Fault is 0.44 g (Walters et al., 2006). This can be equated to a Modified Mercalli Scale intensity VIII. This was represented in the model by horizontal seismic forces. These are shear forces as normal forces do not generate the high residual pore pressures that destabilise the slopes (Finn, 2003). The forces are considered to be positive in the direction of failure by the model. The orientation of the ground acceleration was also the same orientation, assumed in the direction of slope increasing in depth (see figure 3).

The minimum factor of safety was found to be 0.3 for the slope, with the rest of the slope being at a similar value (figure 15). This shows that an event of this magnitude would be more than sufficient to cause failure of the slope.

The implication of this result is that there will be a major landslide in the event of an estimated maximum magnitude Hope Fault earthquake.

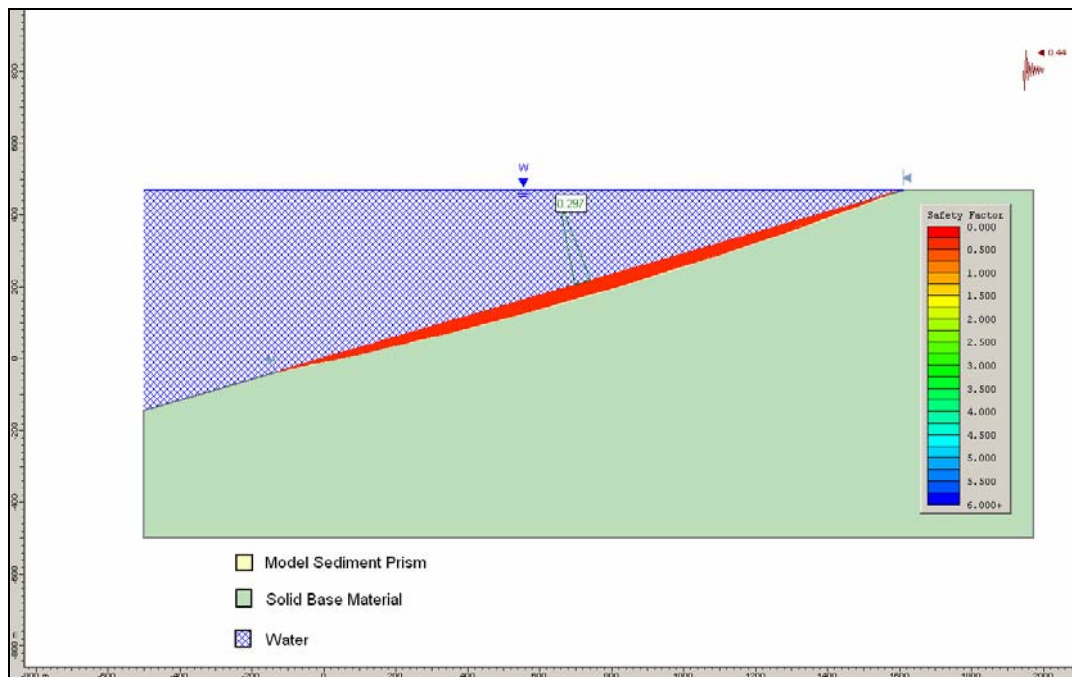


Figure 15 Average Slope in SLIDE 5.0 With Circular Tapered Deposit Profile – 0.44g Seismic Force

### 4.2.3 Deterministic Failure Event Analysis

Since the maximum predicted ground acceleration yields a failure mode in the slope, minimum ground acceleration needed to cause slope failure is also of interest. This is found from determining the ground acceleration that gives a minimum slope surface safety factor of 1.

A series of runs were performed obtaining values of the Seismic Force and the corresponding Minimum Safety Factor for the failure surfaces. This data was then plotted, and the required value of the seismic force required to induce a factor of safety of 1 was interpolated from the graph (see figure 16).

**Table 1 Seismic Force and Minimum Safety Factor Relationship**

Seismic Force	Minimum Safety Factor
0	2.245
0.022	1.836
0.044	1.544
0.066	1.327
0.088	1.157
0.11	1.022
0.132	0.912
0.154	0.821
0.176	0.742
0.198	0.676

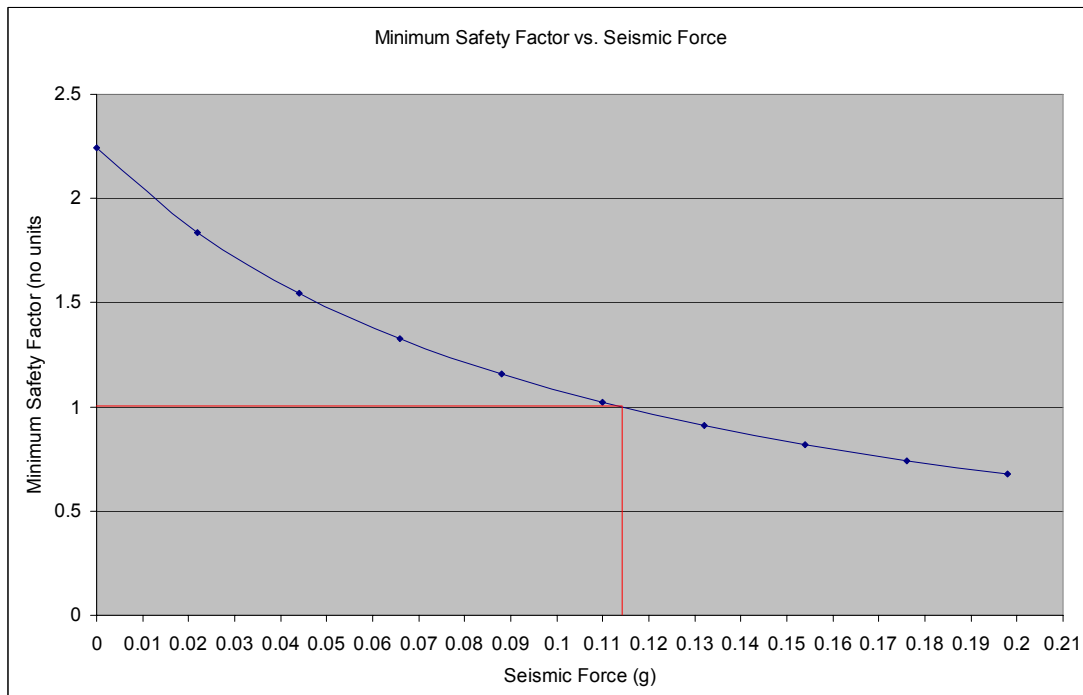


**Figure 16 Interpolated Relationship Between Seismic Force and Minimum Factor of Safety**

This shows that the rate of reduction in safety factor decreases with an increase of seismic force. The value obtained from this plot was a ground acceleration of 0.11 g (rounded from 0.114 g). This is ~25% of the estimated maximum potential ground acceleration produced by the inferred maximum seismic event (Walters et. al., 2006). As many factors affect the seismic performance there can be no exact correlation made between ground acceleration and Moment Magnitude. A reason for this is that there are a large number of factors that can modify the seismic energy before it reaches the ground. The Modified Mercalli energy is the surface effect which is an attenuation of the energy released at the earthquake source as it travels. As this model is simulating a slide initiated by surface ground acceleration, the seismic force relates closely to the Modified Mercalli Intensity. An approximation can be made based on the relationship given in table 2.

**Table 2 Modified Mercalli Intensity to Peak Ground Acceleration (PGA) Relationship (Mitalski 2006)**

Modified Mercalli Intensity	PGA (g)
IV	0.03 and below
V	0.03 - 0.08
VI	0.08 - 0.15
VII	0.15 - 0.25
VIII	0.25 - 0.45
IX	0.45 - 0.60
X	0.60 - 0.80
XI	0.80 - 0.90
XII	0.90 and above

From this table, the approximate size earthquake that would cause failure of the slope is an event that will generate Modified Mercalli Intensity VI at head of the Kaikoura Canyon.

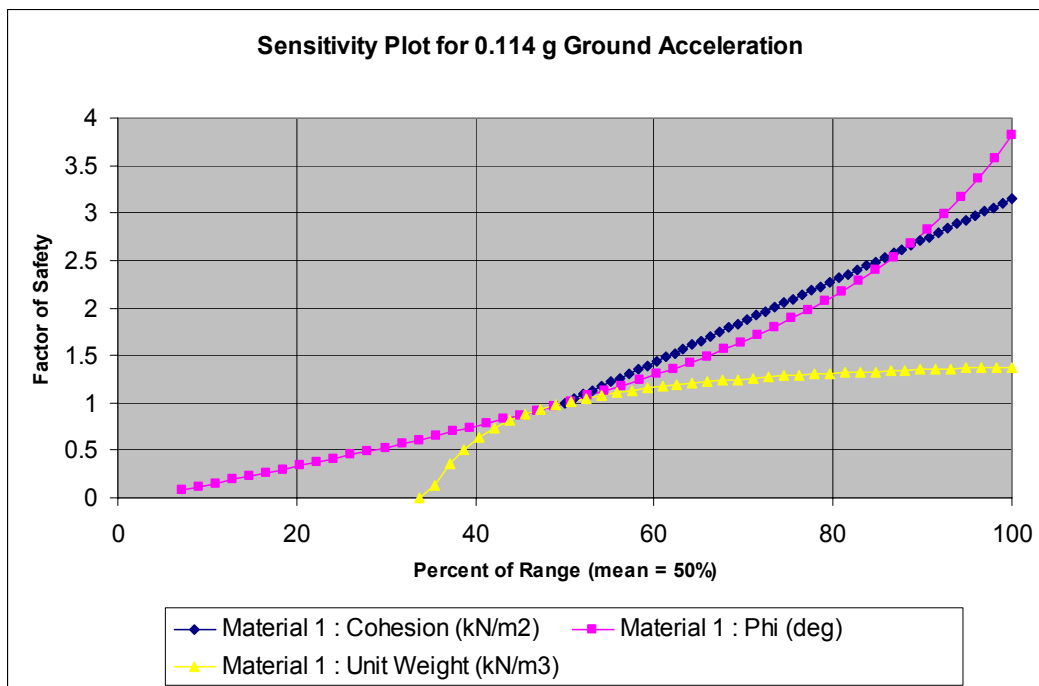
### **4.3 Sensitivity analysis**

A sensitivity analysis was carried out to analyse the uncertainty associated with the parameters that were assumed for the model. This is done by specifying a range of values for each of the assumed parameters and assessing the effect of the variability on the factors of safety. This enables the determination of the parameters that need greater consideration and a higher accuracy. It also helps determine the parameters that have the least effect on the slope, as well as seeing how the soil behaves when a change is induced that affects one of the parameters.

The first sensitivity analysis was performed using a seismic force of 0.11 g, which was the critical ground acceleration needed to induce slope failure. The range of values for which the sensitivity analysis was done were arbitrary, but within ranges that would occur for that parameter in nature, shown in table 3. The results from the sensitivity analysis are shown in figure 17.

**Table 3 Chosen Ranges of Values of the Model Parameters for Sensitivity Analysis**

	Modelled Value	Specified Minimum	Specified Maximum
Cohesion (kN/m <sup>2</sup> )	0	0	5
Phi (°)	33	30	35
Unit Weight (kN/m <sup>3</sup> )	15.696	12	18

**Figure 17 Sensitivity Plot for 0.114g Seismic Force on Average Slope**

The results show that below a critical value for the unit weight of the material ( $\approx 15$  kN/m<sup>3</sup>, which is close to the value that was assumed for the soil) the factor of safety is influenced significantly, with values below  $\approx 10$  kN/m<sup>3</sup> not even registering a value. Values above the assumed unit weight for the material did not have a significant influence, and appeared to trend towards a limit.

The cohesion had a positive linear relationship with the factor of safety. Due to the cohesion having a value of 0 kN/m<sup>2</sup> for the model, there was no lower-bound sensitivity to analyse. The parameter with the greatest sensitivity was the angle of internal friction (phi). The increase in phi showed a growing increase in factor of safety. Both of these results follow the natural characteristics and behaviour of soils in nature. Overestimating the angle of internal friction could render a result of an apparently stable slope which may be potentially unstable.

Changing the ranges of values chosen for the sensitivity analysis for each parameter gauged the importance of the range of values chosen. It showed that the ranges chosen for both the unit weight and cohesion had negligible effect on the sensitivity. There was a slight variation in the sensitivity shown by the angle of internal friction, but this was small

compared to the change in range of values. This meant that the sensitivity results for a ground acceleration of 0.11 g were valid for ranges of upper and lower-bound parameter values. The mean of the percentage change plots was the value selected for the parameter in the model.

As the model was concerned with the effect of varying seismic force, the sensitivity analysis was used to deduce the effect of change in seismic force on the sensitivity for each parameter. This was done by changing the ground acceleration and comparing the sensitivity results from each scenario (figures 18-20).

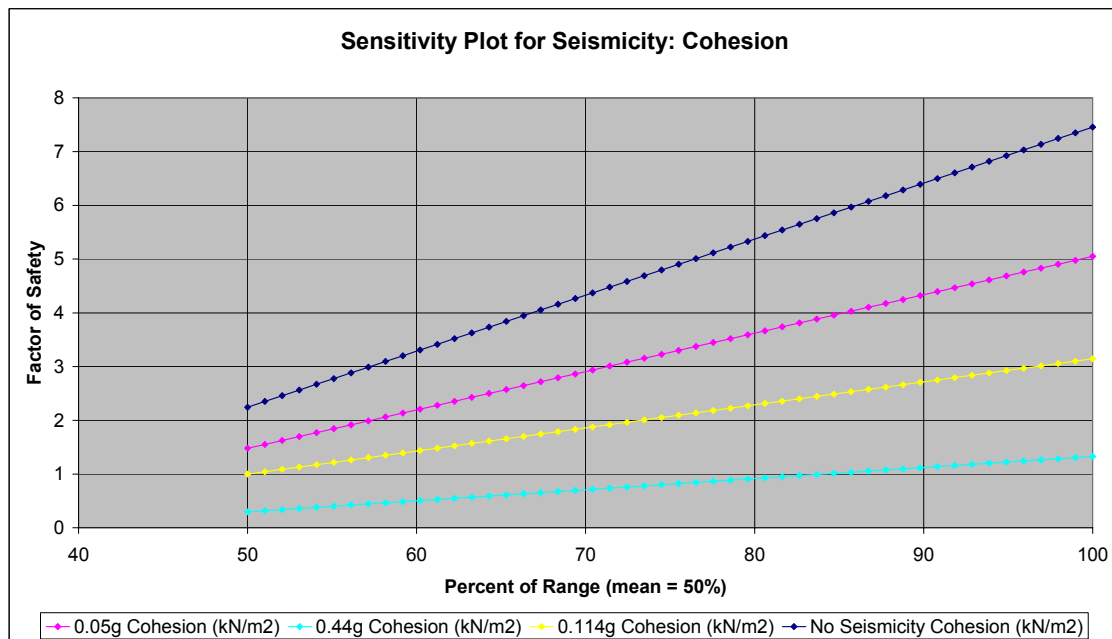


**Figure 18 Sensitivity Plot for Seismic Force and Cohesion Relationship**

The sensitivity of the cohesion parameter appeared to reduce with an increase in seismic force, keeping the same linear relationship. The amount of increase from the minimum value to the maximum value of factor of safety was approximately the same proportion for each of the seismic force inputs ( $\approx 30\%$  increase). This means that more highly cohesive soils, or soils which would act with apparent cohesion during failure, would have more stability.

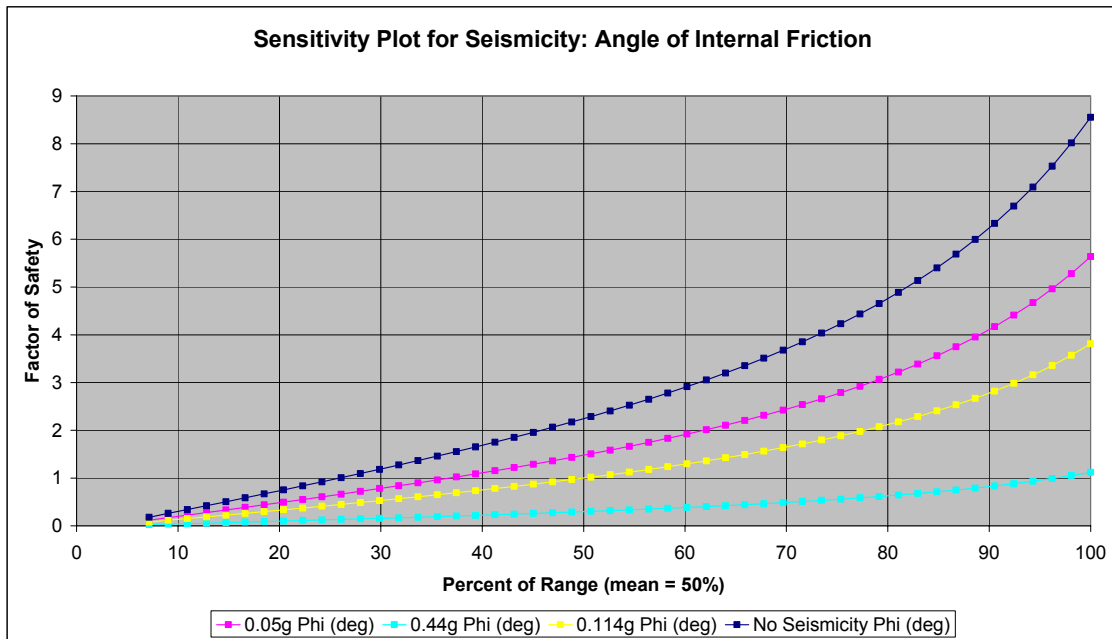


Figure 19 Sensitivity Plot for Seismic Force and Angle of Internal Friction Relationship

The sensitivity of the angle of internal friction followed the same pattern, showing that an increase in ground acceleration gave a reduction in sensitivity. The rate of change of sensitivity also reduced over the specified range of values. This also indicates that the slope would be more stable if the angle of internal friction was higher.

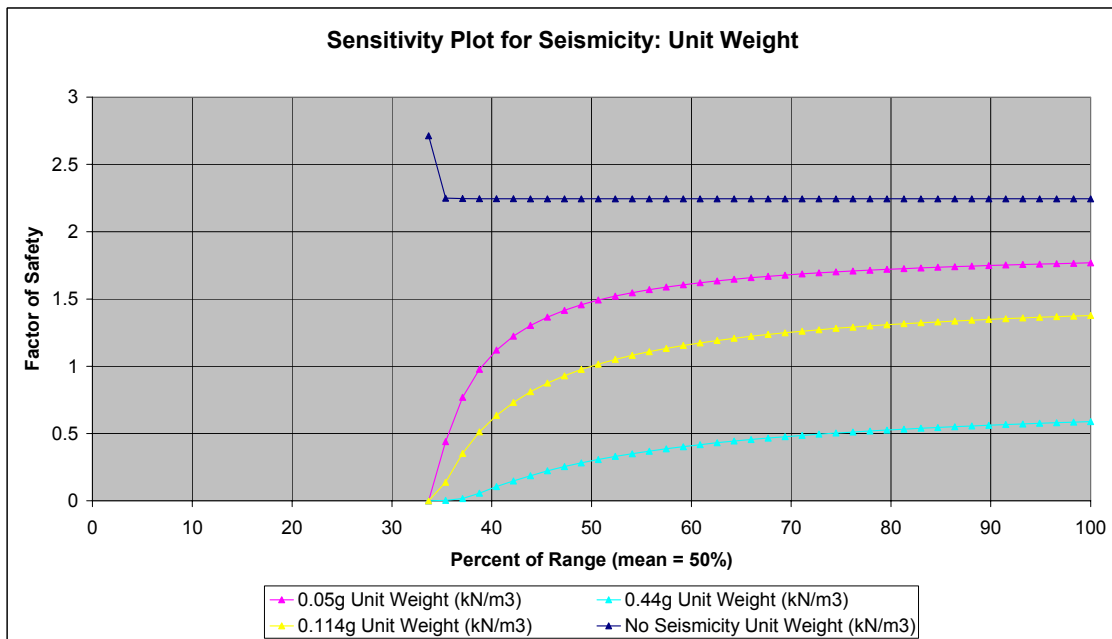


Figure 20 Sensitivity Plot for Seismic Force and Unit Weight Relationship

The overall reduction in sensitivity was the same for the unit weight, excepting that the scenario with no seismic energy present did not start at a safety factor of zero. This indicates that the slope would be more stable with a denser soil.

The effect of varying the ranges was examined by extending the ranges for the soil parameters and analysing the change in sensitivity (see Appendix D). There was negligible increase sensitivity for unit weight and cohesion. There was an increase in sensitivity in the angle of internal friction for the upper-bound values and a reduction for the lower-bound values for the angle of internal friction.

#### 4.4 Variation in Slope

Comparison of the different slopes shows that there was a reasonable amount of slope variation across the sediment deposit. A true representation of the slope would be difficult to model as different parts of the deposit may behave differently due to the observed slope differences. One of the assumptions that was therefore necessary was that the average slope for the whole sediment deposit was representative. To test the validity of this assumption, the same conditions that governed the inputs for the slope were applied to different slopes within the delineated range from the bathymetric map.

The slope around the basin changed from a minimum delineated slope of 1:4.77 to 1:2.54, which equates to almost a doubling of the gradient. This had a significant effect on the stability of the slope, with the factor of safety ranging from 1.7 for the steepest cross-section to 3.1 for the shallowest cross-section. This was for slope without seismic loading. The implication this had on the response to seismic energy was failure of the steepest slope with a ground acceleration of 0.08g which relates to a Modified Mercalli Intensity V event. This is in comparison to the required ground acceleration of 0.2 which relates to a Modified Mercalli Intensity VII event for the average. All of the slopes failed under the predicted maximum ground acceleration of 0.44 g.

As there is quite a variation in slope and consequently stability within the deposit, it therefore follows that the slope can fail in different localised sections depending on the slope gradient, with steeper slopes failing under weaker seismic inputs. This means that the slope can be categorised into failure zones depending on the different ground accelerations.

The zones were established by applying a ground acceleration equal to the upper-bound value for each of the ground accelerations in table 3 for each of the slopes. This indicated which of the areas had failed given the level of seismic force. The result is shown in table 4.

**Table 4 Zones of Failure and the Relationship to Modified Mercalli Intensity and Ground Acceleration**

Modified Mercalli Intensity	Max PGA (g)	Slope 1	Slope 2	Slope 3	Slope 4	Slope 5	Slope 6	Slope 7
IV	0.03							
V	0.08	Failure						
VI	0.15	Failure	Failure					
VII	0.25	Failure						

The slopes which fail at the corresponding ground acceleration are shown in figure 20.

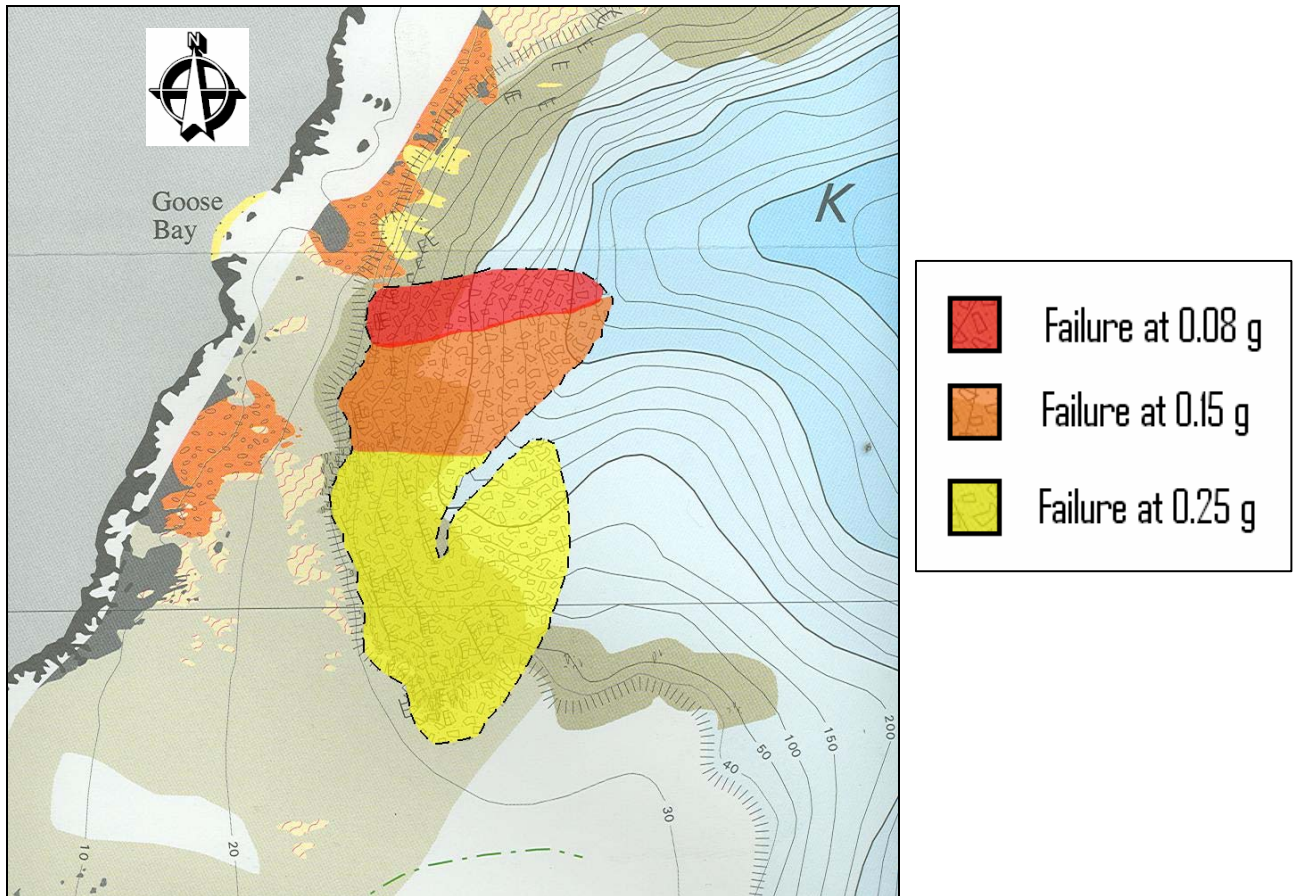


Figure 21 Zones of Varying Stability Within the Sediment Deposit (From Table 4)

This shows that the slopes more susceptible to failure are at the northern flank of the deposit due to the steeper gradient in that area.

## 5.0 Discussion

This study looks at the displacement of sediment caused by seismic activity in the submarine faults (North Canterbury shelf, Conway Ridge and the Keekerengu Bank thrust faults) and submarine landslide.

My project was concerned with the conditions under which the submarine landslide will eventuate. The study by Walters et al, (2006) shows there is a strong possibility of devastating tsunami being generated if the entire slope can fail at once. In addition, the displacement caused by the faults could be from vertical displacement of the ocean floor rather than the energy transmission causing shaking, the latter of which is the scope of my project.

Due to the relatively shallow nature of the deposit, it is likely that in a seismic event that generates the critical ground acceleration leading to failure, the whole slope will fail simultaneously. This does not rule out the possibility of localised failures given at sub-critical ground accelerations.

The results for the stability analysis indicate that the slope, although stable, is susceptible to failure from a ground acceleration that is much less than the estimated probable maximum.

The sensitivity analysis showed that the slope stability was strongly influenced by the cohesion and the angle of internal friction, and was not influenced greatly by the unit weight. Even though fine silts and sand are generally cohesionless, the perturbed soil might not act in this way. Furthermore, the effect of the ground acceleration may induce changes in pore pressure within the sediment. This may make the deposit more unstable than the originally assumed drained behaviour.

The sensitivity of the soil properties showed behaviour that coincided with characteristic behaviour that would be observed in natural soil. This was shown by an increase in stability with an increase cohesion or angle of internal friction.

The sensitivity of the parameters used in the sensitivity analysis was small within the ranges of values that would normally be used for the soil properties for cohesion and unit weight. This means that the results are valid for the values selected, as well as for values that are within the reasonable ranges for the soil properties in nature for these two properties. The angle of internal friction showed a reasonable amount of sensitivity, which shows uncertainty with this model parameter that needs to be researched more. This will give a value that is more specific to the sediment in the model and will give a more accurate representation of the slope failure.

Further validation of this result should be carried out with different modelling programs. Other programs, such as 2D SEDFLUX which can be used to examine the location and attributes of sediment failure along continental margins, may be able to be used to simulate the same scenario (Syvitski 2003). This examines the effects of sediment grain size, sea floor bathymetry, ocean energy and sea level. There are also models like BING which incorporate the yield strength of the material (Imran 2001). The modelling of the

slope with other programs would give a results based on other slope parameters that may affect the slope stability.

There are many other factors that may contribute to slope instability. The high resolution seismic profiling showed evidence of accumulation of small amounts of gas in the sediment (Lewis & Barnes 1999) which may act as a triggering mechanism for slope failure or instability (Sultan et al., 2004). Cyclical seismic loading can cause the vertical effective stress in loose sands to reduce to zero causing liquefaction, as well as some clayey soils being very sensitive to disturbance with a significant loss of strength (Sultan et al., 2004).

Because of the potentially devastating effects from tsunami coupled with the strong likelihood of mass slope failure, steps into hazard mitigation need to be taken. This is especially critical for the Oaro area. As there will be an extremely short amount of time between the slope failure and the generation of a tsunami there will be limited warning signs of the impending swell. These signs may be in the form of an earthquake event or receding shoreline.

## **6.0 Conclusions and Recommendations**

- In the paper by Walters et al. (2006) it states that there will be a significant threat from tsunami caused by the displacement of 0.24 km<sup>3</sup> of sediment in the Kaikoura Canyon. This was found by computer modelling of the effect from the sediment deposit identified in this report suffering a catastrophic failure and developing a tsunami of up to 12 m in height. It also estimates a potential ground acceleration of 0.44g in the Kaikoura region.
- The unperturbed slope is stable. The steepest section of the slope, without seismic loading, has a safety factor of 1.7.
- Some of the sediment could be displaced with a ground acceleration of 0.08 g, which correlates to a Modified Mercalli Intensity V.
- The critical ground acceleration for failure of the whole slope is 0.2 g.
- The slope sections will fail as a unit at 0.2 g
- The slope may have independent failure in different places depending on the amount of ground acceleration the slope is subjected to.
- Further validation of the findings using other slope stability analyses is needed to confirm the potentially unstable nature of the slope and the outcome of slope failure.
- As slope failure is likely to occur due to predicted amounts of ground acceleration there is a significant tsunami hazard in the area. Hazard mitigation steps need to be prepared for the areas that may be affected by a tsunami being generated from submarine landslide in the Kaikoura Canyon.

## **7.0 Acknowledgements**

I would like to thank Tim Davies my supervisor and Tom Cochrane the course coordinator. I would also like to thank Bob and Margaret Stewart for their support and encouragement throughout this project.

## 8.0 References

Bowman, E, pers comm., June 6, 2006.

Carter, L. and Herzer, R.H. (1979) *The Hydraulic Regime and its Potential to Transport Sediment on the Canterbury Continental Shelf*. New Zealand Oceanographer, Vol. 83, 33

Davies, Tim, pers comm., March 23, 2006.

Denlinger, Roger P. and Iverson, Richard M. (2001). *Flow of variably fluidized granular masses across three-dimensional terrain 2. Numerical predictions and experimental tests*. Journal of Geophysical Research, Vol. 106, No. B1, Pages 553–566, Jan 10, 2001

van Dissen, R and Yeats, R. (1991). *Hope fault, Jordan thrust, and uplift of the Seaward Kaikoura Range, New Zealand*. Geology: Vol. 19, No. 4, pp. 393–396.

Fisher, M, Normark, R, Greene, H, Lee, H, and Sliter, R. (2005). *Geology and tsunamigenic potential of submarine landslides in Santa Barbara Channel, Southern California*. Marine Geology 224 (2005) 1– 22

Freund, R (1971) *The Hope Fault: A Strike Slip Fault in New Zealand*. New Zealand Geological Survey, Bulletin 86. New Zealand Department of Scientific and Industrial Research.

Grilli, S.T. and P. Watts. (2005). *Tsunami generation by submarine mass failure Part I : Modeling, experimental validation, and sensitivity analysis*. Journal of Waterway Port Coastal and Ocean Engineering., 131(6), 283-297.

Hayir, A. (2006). *The near-field tsunami amplitudes caused by submarine landslides and slumps spreading in two orthogonal directions*. Ocean Engineering 33 (2006) 654–664

Hayir, A (2003). *The effects of variable speeds of a submarine block slide on near-field tsunami amplitudes*. Ocean Engineering 30 (2003) 2329–2342.

Imran, J., Harff, P., and Parker G. (2001) *A Numerical Model of Submarine Debris Flow with Graphical User Interface*. Computers and Geosciences 27, 717-729.

de Lange WP, Fraser RJ (1999). *Overview of tsunami hazard in New Zealand*. Tephra 17:3–9

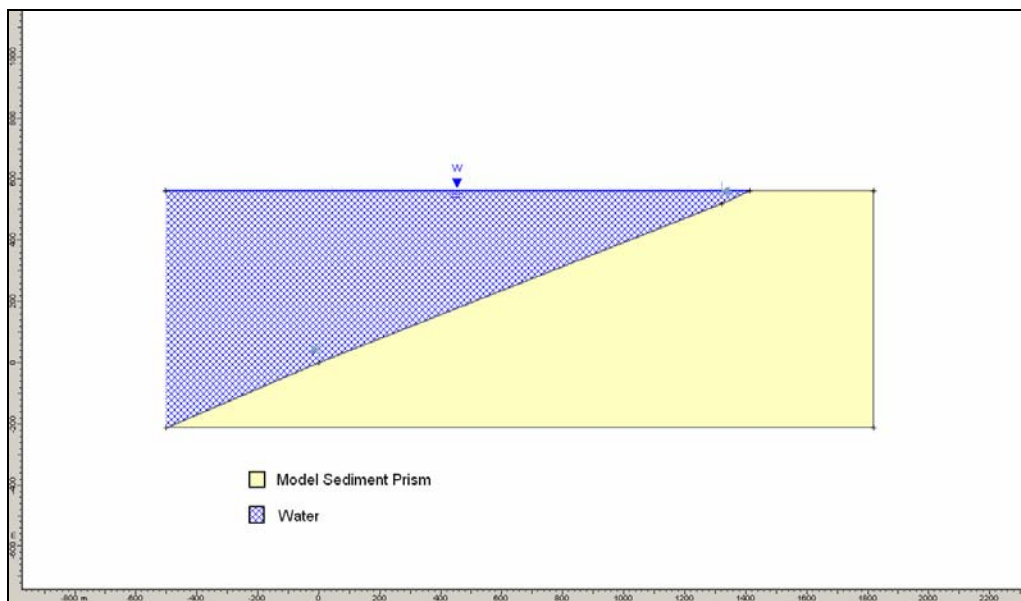
Lewis, K. B., and Barnes, P, M., (1999) *Kaikoura Canyon, New Zealand: active conduit from near shore sediment zones to trench-axis channel*. Marine Geology 162: 39-69.

- Liu PL-F, Wu T-S, Raichlen F, Synolakis C.E, Borrero J.C. (2005). *Run-up and run-down generated by three-dimensional sliding masses*. Journal of fluid Mechanics 536: 107–144
- Mitalski, Marc (2006). *Measuring and Recording Intensity, Magnitude, Energy and Acceleration*. Architectural Registration Exam Workshops [Online]. Available: www.prepa-r-e.com [2006, September 20]
- Pitman, E, Nichita, C, Patra, A, Bauer, A, Sheridan, M, and Bursik, M. (2003). *Computing granular avalanches and landslides*. Physics of Fluids Volume 15, No 12 December 2003.
- Pitman, E, Patra, A. and Bauer, A. (2002) *Computing Debris Flows and Landslides*. The University at Buffalo, Buffalo New York.
- Robinson, R., (2004) *Potential earthquake triggering in a complex fault network: the northern South Island, New Zealand*. Geophysical Journal International Volume 159 Page 734
- Stirling, M., McVerry, G. and Berryman, K. (2002) *A New Seismic Hazard Model for New Zealand*. Bulletin of the Seismology Society of America, Vol 92, No. 5, pp 1878-2002.
- Stirling, M., Pettinga J.R., Berryman, K. and Yetton, M.D. (2001) *Probabilistic seismic hazard assessment of the Canterbury Region, New Zealand*. Bulletin of the New Zealand Society for Earthquake Engineering 34: 318-334.
- Sultan N., Cochonat, P, Canals, M, Cattaneo,A, Dennielou, B, Hafliadason, H, Laberg,J.S, Long, D, Mienert, J, Trincardi, F, Urgeles, R, Vorren T.O, and Wilson, C. (2004) *Triggering mechanisms of slope instability processes and sediment failures on continental margins: a geotechnical approach*. Marine Geology December 2004; 213(1-4) : 291-321
- Syvitski, J.P., and Hutton, E.W., (2003) *Failure of Marine Deposits and their Redistribution by Sediment Gravity Flows*. Pure Applied Geophysics, 160, 2053-2069
- Todorovska, M.I, Hayir, A, and Trifunac, M.D (2002) *A Note on Tsunami Amplitudes Above Submarine Slides and Slumps*. Soil Dynamics and Earthquake Engineering 22 (2002) 129-141.
- Trifunac, M.D, and Todorovska, M.I. (2002). *A Note on Differences in Tsunami Source Parameters for Submarine Slides and Earthquakes*. Soil Dynamics and Earthquake Engineering 22 (2002) 143-155.
- Walters, R, Barnes, P, Lewis, K, Goff, J and Fleming, J. (2006). *Locally generated tsunami along the Kaikoura coastal margin: Part 2. Submarine landslides*. New Zealand Journal of Marine and Freshwater Research, 2006, Vol. 40: 17–28

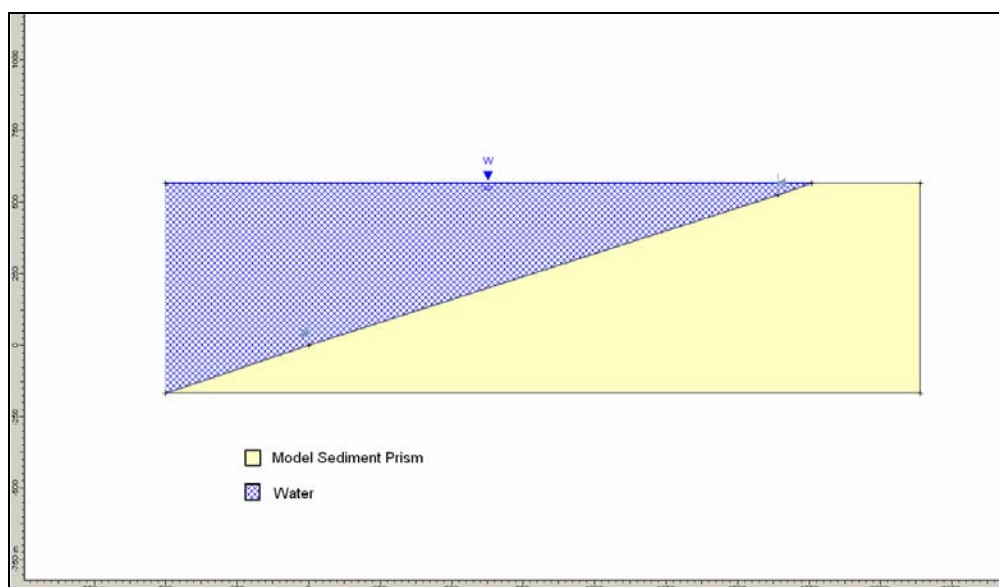
- Walters, R, Barnes, P, and Goff, J. (2006) *Locally generated tsunami along the Kaikoura coastal margin: Part 1. Fault ruptures*. New Zealand Journal of Marine and Freshwater Research, 2006, Vol. 40: 1–16.
- Watts, P, Imamura, F and Grilli, S. (2000) *Comparing Model Simulations of Three Benchmark Tsunami Generation Cases*. Journal of Science Tsunami Hazards, 18(2), 107-123.
- Wright, S.G., and Rathje, E.M. (2003). *Triggering Mechanisms of Slope Instability and their Relationship to Earthquakes and Tsunamis*. Pure Applied Geophysics, 160, 1865-1877.

## 9.0 Appendices

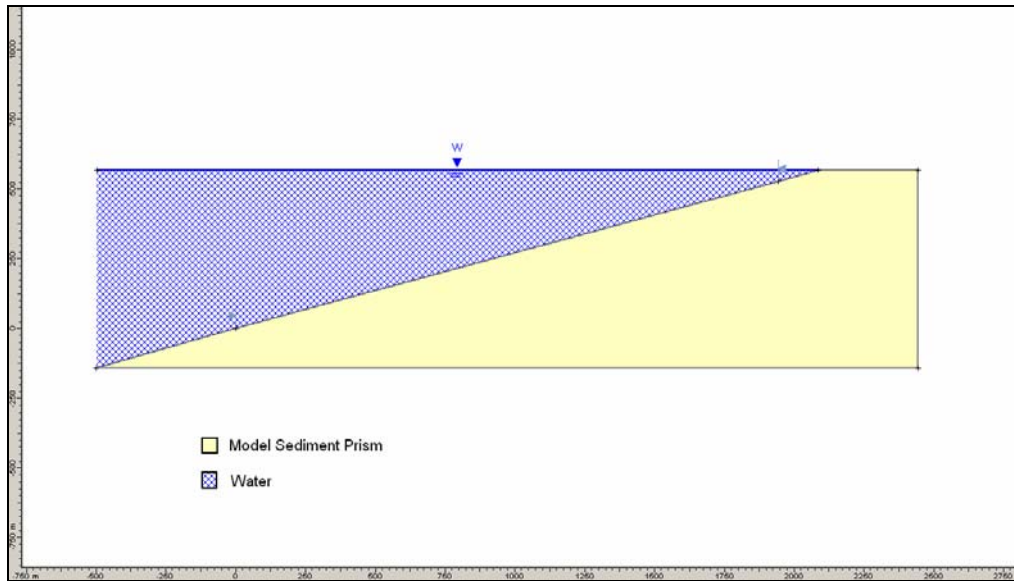
### Appendix A *Slope Delineations From Bathymetric Contours for Cross-Sections*



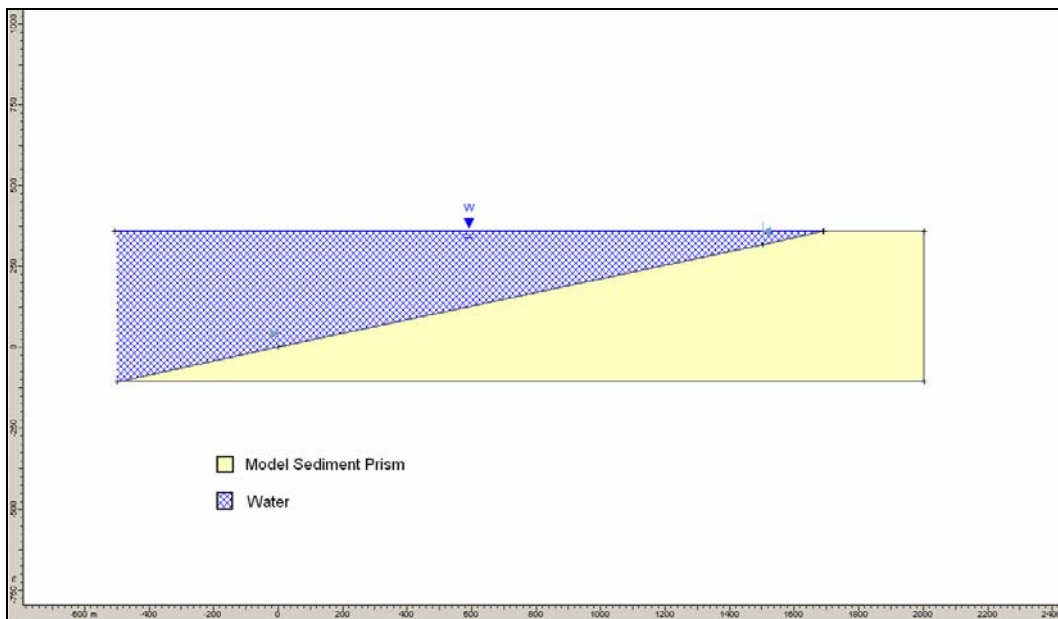
**Cross-section 1**



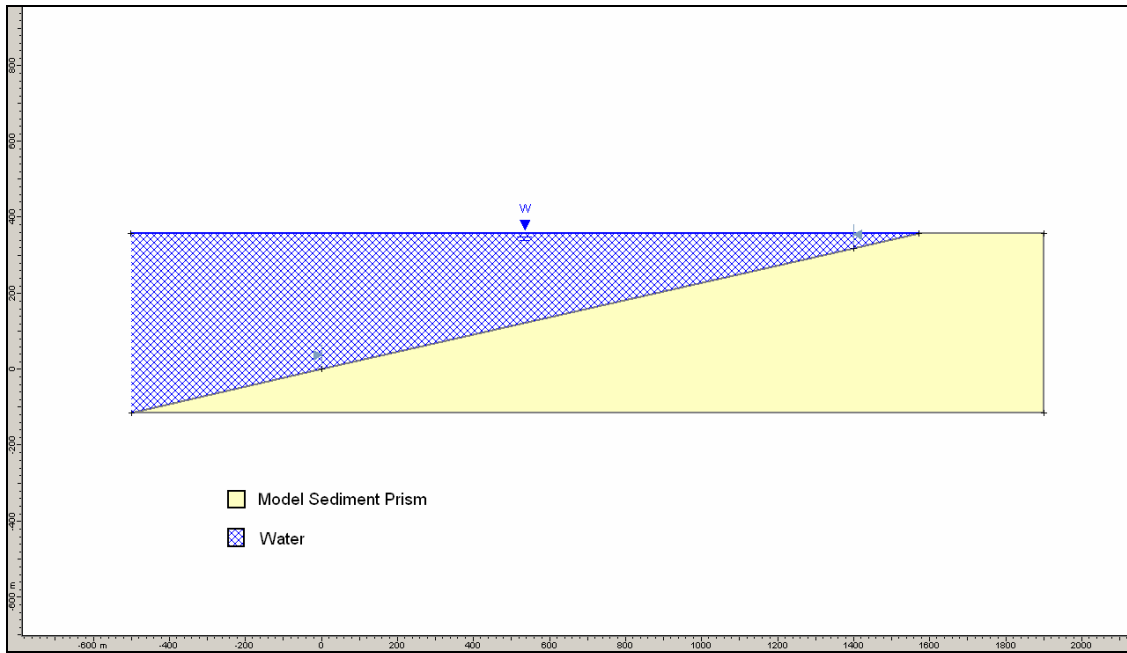
**Cross-section 3**



**Cross-section 4**



**Cross-section 5**

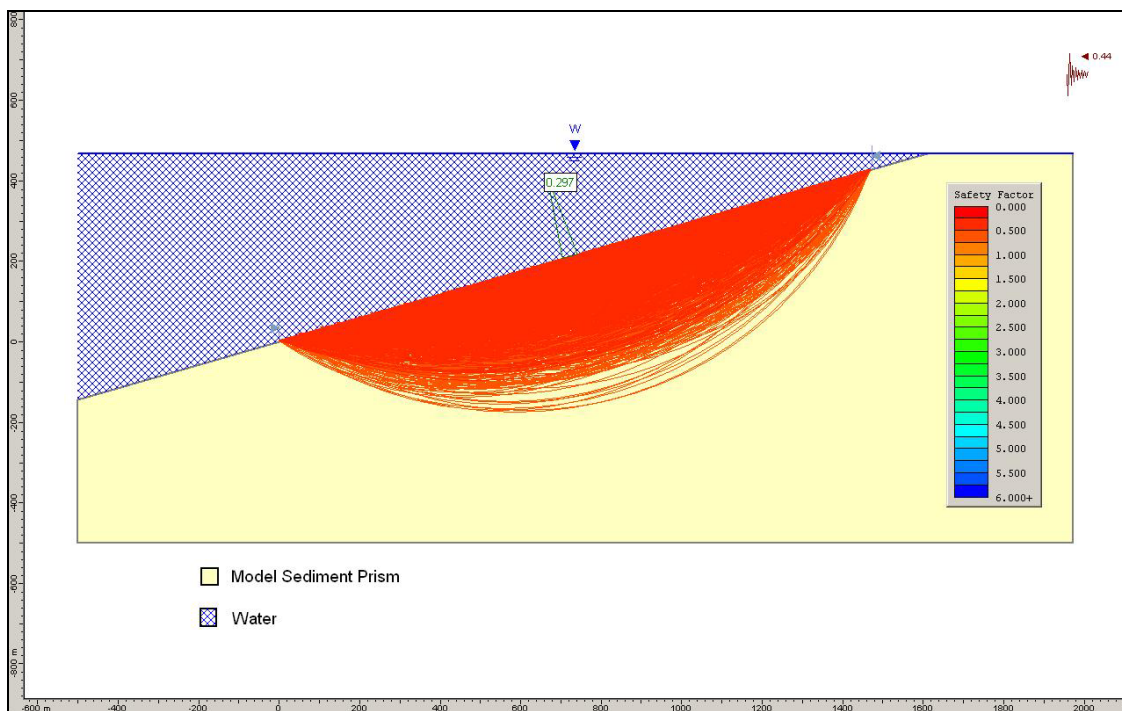


**Cross-section 7**

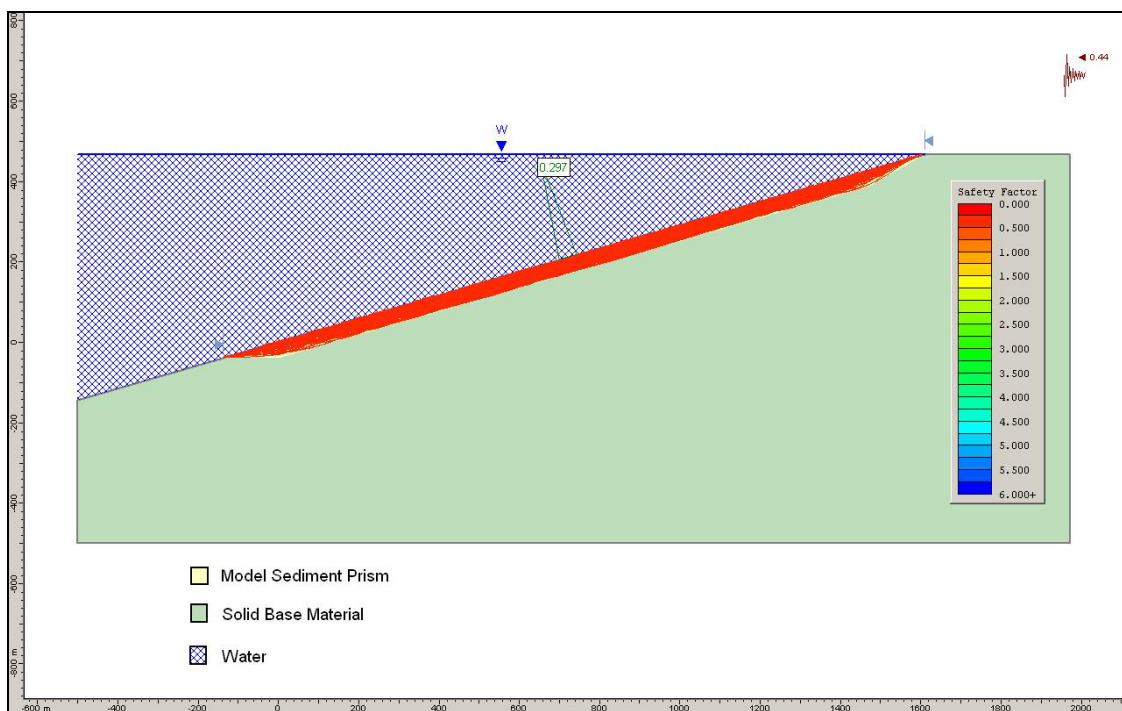
**Appendix B Table of Contour Delineation Values for Sediment Prism**

		Distance from Sediment Prism Base Point to Contours for Each Site						
		1	2	3	4	5	6	7
Depth Below Mean Sea Level (m)	-575	0	0	0	0			
	-550	80	88	88	88			
	-500	208	240	292	320			
	-450	320	400	448	496			
	-400	476	520	548	612			
	-360	-	-	-	-	0	0	0
	-350	552	628	664	784	48	52	44
	-300	680	740	756	920	344	312	276
	-250	796	816	852	1108	564	548	512
	-200	880	944	1040	1392	688	648	664
	-150	992	1128	1272	1568	1080	924	736
	-100	1164	1252	1400	1672	1228	1148	952
	-50	1284	1356	1596	1876	1412	1500	1220
	-40	1320	1392	1640	1944	1504	1596	1400
Site	1	2	3	4	5	6	7	Average
Average Slope	0.405303	0.384339	0.32622	0.275206	0.212766	0.200501	0.228571	0.290415
Horizontal Slope Length	1320	1392	1640	1944	1504	1596	1400	1542.286

### Appendix C Model Outputs for Homogeneous & Uniform Soil Profile Slopes Under Different Ground Acceleration Conditions



Average Slope in SLIDE 5.0 With Homogeneous Deposit Profile – 0.044g Seismic Force



Average Slope in SLIDE 5.0 With Uniform Deposit Profile – 0.044g Seismic Force

### Appendix D Change in Sensitivity of Model Parameters Given a Change of Sensitivity Range

